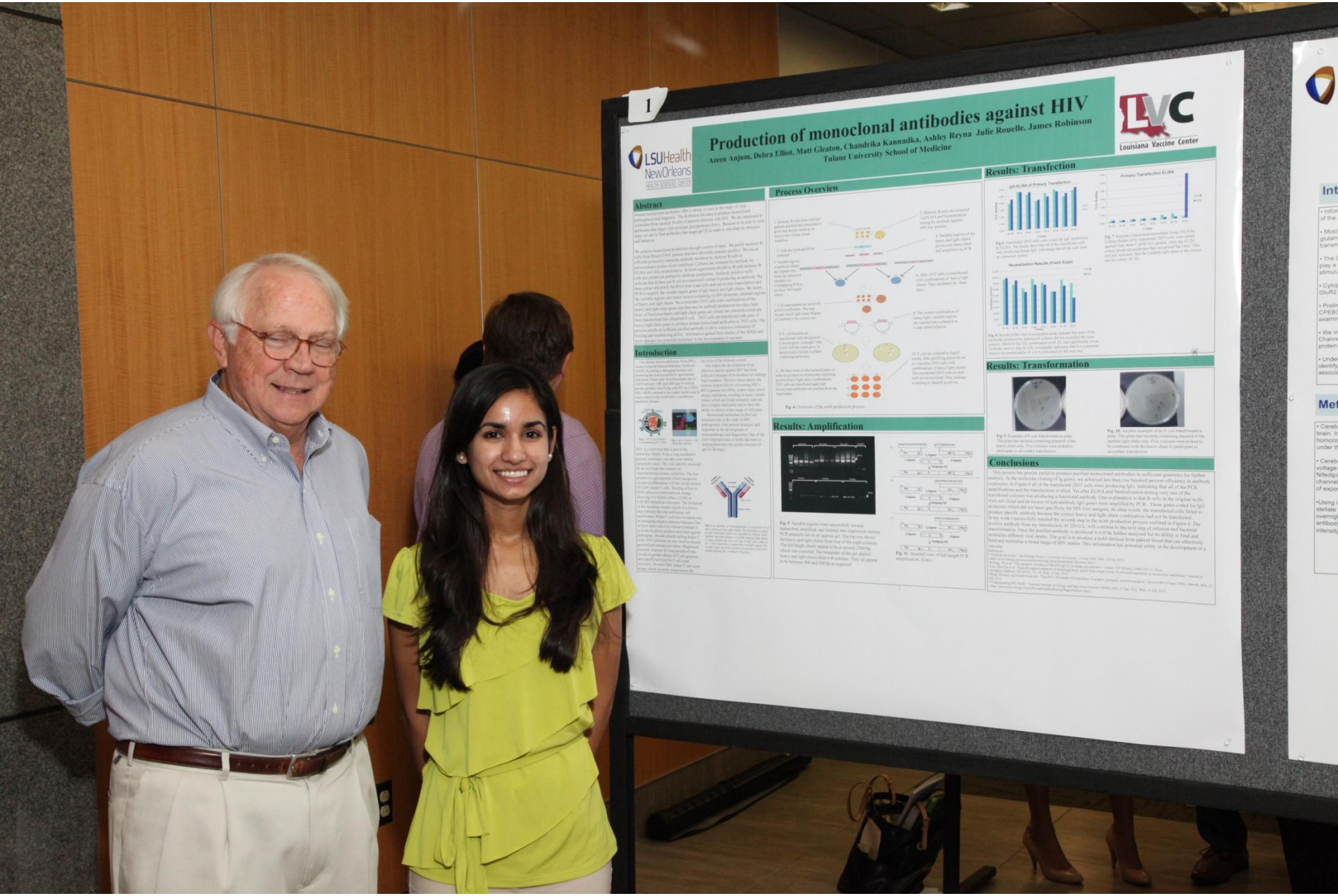
1
Production of monoclonal antibodies against HIV
Azeen Anjum, Debra Elliot, Matt Gleaton, Chandrika Kannadka, Ashley Reyna Julie Rouelle, James Robinson
Tulane University School of Medicine
LSUHealth NewOrleans
HEALTH SCIENCES CENTER
LVC
Louisiana Vaccine Center
Abstract
Introduction
Process Overview
Results: Amplification
Results: Transfection
Results: Transformation
Conclusions

2

LSUHealth NewOrleans HEALTH SCIENCES CENTER

Cellular mechanisms of activity dependent regulation of CPEB3 expression in mouse cerebellar stellate cells

Khaled Badr, Crhistian Bender, June Liu

Department of Cell Biology and Anatomy, LSU Health Science Center, New Orleans, LA 70112

PATRICK F. TAYLOR FOUNDATION

Introduction:

• Information processing in the central nervous system is based on the balance of the actions of excitatory and inhibitory neurons.

• Most excitatory neurons use glutamate as their neurotransmitter. AMPA type glutamate receptors are essential for moderating this excitatory synaptic transmission.

• The GluR2 subunit of AMPA receptors (AMPARs) in cerebellar stellate cells play a key role in associative learning and memory. A single fear-inducing stimulus causes an increase in GluR2-containing AMPARs.

• Cytoplasmic Polyadenylation Element Binding protein 3 (CPEB3) regulates GluR2 synthesis and is associated with learning and human episodic memory.

• Preliminary study in our lab show that action potential (AP) firing increases CPEB3 expression and reduces synaptic GluR2 receptors. Therefore, we examined the mechanism that regulates CPEB3 expression.

• We investigated 1) the role of calcium entry via Voltage Gated Calcium Channels (VGCC) during spontaneous action potential firing; 2) its effect on protein synthesis and protein degradation of CPEB3.

• Understanding the mechanism that regulates CPEB3 expression helps in identifying mechanisms that regulates GluR2 and hence, the neuroplasticity associated to this receptor.

Methods:

• Cerebellar cell cultures were prepared from postnatal day 7 (P7) mouse brain. In order to identify cerebellar stellate cells, we used a strain of homorozygous transgenic mice expressing green fluorescent protein (GFP) under the control of the glutamic acid decarboxylase 65kDa promoter.

• Cerebellar cells were incubated with a sodium channel blocker (TTX), voltage-gated calcium channel inhibitors (NNC 55-0396 dihydrochloride, Nifedipine, and ω-Conotoxin, which blocks T-type, L-type, and N-type calcium channel, respectively) and a proteasome inhibitor (MG132). After three hours of exposure to drugs, the cells were fixed for twenty minutes.

•Using immunocytochemistry, we measured CPEB3 levels. The cerebellar stellate cells were incubated with rabbit anti-CPEB3 primary antibody overnight and then with a red fluorescent donkey anti-rabbit IgG secondary antibody for one hour. The cells were then photographed and the fluorescence intensity was quantified in each individual GFP positive cell.

TTX causes a decrease in CPEB3 expression levels

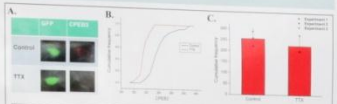

Figure 1. (A) Examples of cerebellar stellate cells. Control cells show high expression of CPEB3. TTX treated cells show decreased levels of CPEB3. (B) Experimental cells treated with TTX show leftwards shift in cumulative frequency (Control vs. TTX K-S p= 4.8861E-06) (C) Histogram showing the mean intensity of the control cells and those cells treated with TTX

Voltage-Gated Calcium Channels regulates CPEB3 expression level

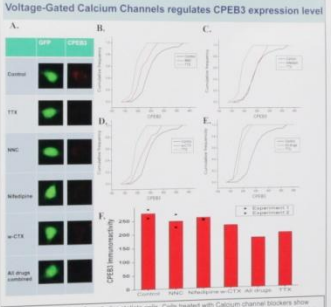

Figure 2. (A) Examples of cerebellar stellate cells. Cells treated with Calcium channel blockers show decreased levels of CPEB3. (B-E) Experimental cells treated with NNC, Nifedipine, ω-CTX, and all of the drugs combined show leftwards shift in cumulative frequency (Control vs. NNC K-S p= 0.000634, Control vs. Nifedipine K-S p=0.014946, Control vs. ω-CTX K-S p=0.002348, Control vs. all drugs combined K-S p=1.25E-10). This shows that CPEB3 expression in the TTX and calcium channel blockers treated cells has decreased significantly, with the exception of cells treated with Nifedipine. (F) Histogram showing the mean intensity of the control cells and those cells treated with TTX and different Ca2+ channel blockers.

TTX presence enhances protein degradation

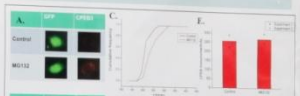

Figure 3. Figure 1. (A, B) Cells treated with proteasome inhibitor MG132 show high expression of CPEB3. TTX + MG132 treated cells show elevated levels of CPEB3. (C, D) Distribution of CPEB3 expression. Experimental cells treated with TTX show leftwards shift in cumulative frequency (K-S p= 0.040379) Experimental cells treated with MG132 and TTX+MG132 show rightwards shift in cumulative frequency (K-S p= 0.02204, K-S p= 0.00226). This suggests that that MG132 completely prevents the TTX-induced reduction in CPEB3 levels. (E, F) Histogram showing the mean intensity

Conclusions:

• Inhibition of action potentials by TTX causes a significant decrease of ~25% in CPEB3 expression in mouse cerebellar stellate cells. Membrane depolarization can activate volt gated calcium channels (VGCC). Here we found that blocking N-, T- and L-type VGCCs each causes a reduction in CPEB3 expression, and inhibition of all three channels redu the CPEB3 levels to that of TTX treatment. Thus voltage-gated calcium channels play role in regulating CPEB3 expression.

• The TTX-induced decrease in CPEB3 expression could result from an enhanced pr degradation or suppression of synthesis of CPEB3 protein. Our preliminary results s MG132 completely prevents the TTX-induced reduction in CPEB3 levels, indicating inhibition of action potential activity increases protein degradation of CPEB3 protei

3

LSUHealth NewOrleans HEALTH SCIENCES CENTER

Effect of Various Synchronization Methods on Gene Expression Profiles in Circadian and Cell Cycle-associated Transcripts

Audrey M. Bell, Tracy L. Mandichak, Aaron E. Hoffman Ph.D
Tulane Cancer Center

Tulane University TULANE CANCER CENTER

Introduction

Materials and Methods

Circadian Genes

Cell Cycle Genes

Conclusions

4

LSUHealth NewOrleans HEALTH SCIENCES CENTER

Rituximab in Pedi... Nephro...

Cierra Bonvillain, D...
Xavier University of Louisiana, Lo...

Abstract

Meth...

Results

Results

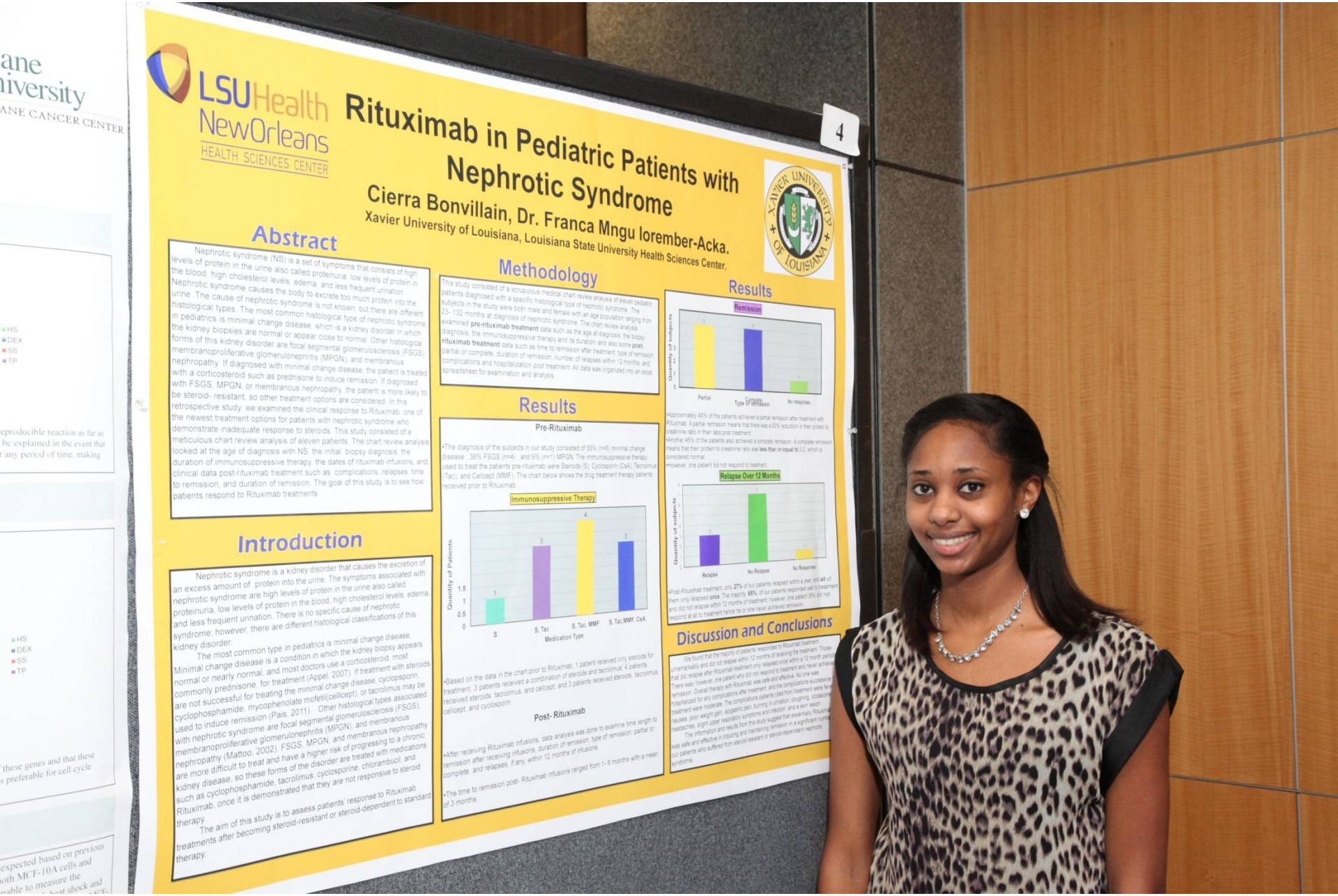
LSUHealth NewOrleans HEALTH SCIENCES CENTER
Rituximab in Pediatric Patients with Nephrotic Syndrome
Cierra Bonvillain, Dr. Franca Mngu lorember-Acka.
Xavier University of Louisiana, Louisiana State University Health Sciences Center.
4
Abstract
Nephrotic syndrome (NS) is a set of symptoms that consists of high levels of protein in the urine also called proteinuria, low levels of protein in the blood, high cholesterol levels, edema, and less frequent urination. Nephrotic syndrome causes the body to excrete too much protein into the urine. The cause of nephrotic syndrome is not known, but there are different histological types. The most common histological type of nephrotic syndrome in pediatrics is minimal change disease, which is a kidney disorder in which the kidney biopsies are normal or appear close to normal. Other histological forms of this kidney disorder are focal segmental glomerulosclerosis (FSGS), membranoproliferative glomerulonephritis (MPGN), and membranous nephropathy. If diagnosed with minimal change disease, the patient is treated with a corticosteroid such as prednisone to induce remission. If diagnosed with FSGS, MPGN, or membranous nephropathy, the patient is more likely to be steroid- resistant, so other treatment options are considered. In this retrospective study, we examined the clinical response to Rituximab, one of the newest treatment options for patients with nephrotic syndrome who demonstrate inadequate response to steroids. This study consisted of a meticulous chart review analysis of eleven patients. The chart review analysis looked at the age of diagnosis with NS, the initial biopsy diagnosis, the duration of immunosuppressive therapy, the dates of rituximab infusions, and clinical data post-rituximab treatment such as: complications, relapses, time to remission, and duration of remission. The goal of this study is to see how patients respond to Rituximab treatments.
Introduction
Nephrotic syndrome is a kidney disorder that causes the excretion of an excess amount of protein into the urine. The symptoms associated with nephrotic syndrome are high levels of protein in the urine also called proteinuria, low levels of protein in the blood, high cholesterol levels, edema, and less frequent urination. There is no specific cause of nephrotic syndrome; however, there are different histological classifications of this kidney disorder.
The most common type in pediatrics is minimal change disease. Minimal change disease is a condition in which the kidney biopsy appears normal or nearly normal, and most doctors use a corticosteroid, most commonly prednisone, for treatment (Appel, 2007). If treatment with steroids are not successful for treating the minimal change disease, cyclopsporin, cyclophosphamide, mycophenolate mofetil(cellcept), or tacrolimus may be used to induce remission (Pais, 2011). Other histological types associated with nephrotic syndrome are focal segmental glomerulosclerosis (FSGS), membranoproliferative glomerulonephritis (MPGN), and membranous nephropathy (Mattoo, 2002). FSGS, MPGN, and membranous nephropathy are more difficult to treat and have a higher risk of progressing to a chronic kidney disease, so these forms of the disorder are treated with medications such as cyclophosphamide, tacrolimus, cyclosporine, chlorambucil, and Rituximab, once it is demonstrated that they are not responsive to steroid therapy.
The aim of this study is to assess patients' response to Rituximab treatments after becoming steroid-resistant or steroid-dependent to standard therapy.
Methodology
This study consisted of a scrupulous medical chart review analysis of eleven pediatric patients diagnosed with a specific histological type of nephrotic syndrome. The subjects in the study were both male and female with an age population ranging from 23- 132 months at diagnosis of nephrotic syndrome. The chart review analysis examined pre-rituximab treatment data such as the age at diagnosis, the biopsy diagnosis, the immunosuppressive therapy and its duration, and also some post-rituximab treatment data such as time to remission after treatment, type of remission: partial or complete, duration of remission, number of relapses within 12 months, and complications and hospitalization post treatment. All data was organized into an excel spreadsheet for examination and analysis.
Results
Pre-Rituximab
•The diagnosis of the subjects in our study consisted of 55% (n=6) minimal change disease , 36% FSGS (n=4) , and 9% (n=1) MPGN. The immunosuppressive therapy used to treat the patients pre-rituximab were Steroids (S), Cyclosporin (CsA), Tacrolimus (Tac), and Cellcept (MMF). The chart below shows the drug treatment therapy patients received prior to Rituximab.
Immunosuppressive Therapy
Quantity of Patients
Medication Type
S
S, Tac
S, Tac, MMF
S, Tac,MMF, CsA
•Based on the data in the chart prior to Rituximab; 1 patient received only steroids for treatment, 3 patients received a combination of steroids and tacrolimus, 4 patients received steroids, tacrolimus, and cellcept, and 3 patients received steroids, tacrolimus, cellcept, and cyclosporin.
Post- Rituximab
•After receiving Rituximab infusions, data analysis was done to examine time length to remission after receiving infusions, duration of remission, type of remission: partial or complete, and relapses, if any, within 12 months of infusions.
•The time to remission post- Rituximab infusions ranged from 1- 6 months with a mean of 3 months.
Results
Remission
Quantity of subjects
Partial
Complete
No response
Type of Remission
•Approximately 45% of the patients achieved a partial remission after treatment with Rituximab. A partial remission means that there was a 50% reduction in their protein to creatinine ratio in their labs post treatment.
•Another 45% of the patients also achieved a complete remission. A complete remission means that their protein to creatinine ratio was less than or equal to 0.2, which is considered normal.
•However, one patient did not respond to treatment.
Relapse Over 12 Months
Quantity of subjects
Relapse
No Relapse
No Response
•Post-Rituximab treatment, only 27% of our patients relapsed within a year, and all of them only relapsed once. The majority, 55%, of our patients responded well to treatment and did not relapse within 12 months of treatment, however, one patient (9%) did not respond at all to treatment hence he or she never achieved remission.
Discussion and Conclusions
We found that the majority of patients responded to Rituximab treatment remarkably and did not relapse within 12 months of receiving the treatment. Those that did relapse after Rituximab treatment only relapsed once within a 12 month period. There was, however, one patient who did not respond to treatment and never achieved remission. Overall therapy with Rituximab was safe and effective. No one was hospitalized for any complications after treatment, and the complications successfully treatment were moderate. The complications patients cited from treatment were fe headaches, slight upper respiratory symptoms and infection, and a skin lesion. nausea, poor weight gain, epigastric pain, burning in urination, coughing, occasional
The information and results from this study suggest that essentially Rituxim was safe and effective in inducing and maintaining remission in a significant numb our patients who suffered from steroid-resistant or steroid-dependent nephrotic syndrome.

LSU Health New Orleans
HEALTH SCIENCES CENTER

In Vivo Model of Glioblastoma

Kenia Carvajal, Mentor: Alberto E. Musto
Neurosurgery and Neuroscience and Cancer Center, Louisiana State University Health Sciences Center

Patrick F. Taylor Foundation

Abstract

Approximately 50% of all patients diagnosed with brain tumors have the most malignant form, Glioblastoma Multiforme (GBM).GBM is aggressive and is characterized by rapid glial cell growth, resistance to radio- and chemo- therapies, and relentless infiltration and spreading throughout the central nervous system (CNS).The purpose of my project was to determine the evolution of GBM size in an in vivo model of Glioblastoma. Balbic nu/nu female mice (5-6 weeks/ 25gm) were randomly selected and 5x10⁵ 5µL mCherry-transduced U87MG human glioblastoma cells were injected under anesthesia in the striatum and the hippocampus guided by stereotaxical approach. Weight, hind limb posture, and locomotive function including gait, grasping reflex, and movement were monitored daily. In vivo fluorescence scan (Zeroigen IVIS-200) was used for detection of intracerebral mCherry U87MG cells in mice every week for six weeks. Then, the resulted signals were quantified using Image J. At the end of experiment, in order to verify the presence of tumors, the animals were sacrificed. The brains were dissected, placed in fixative solutions, sectioned, mounted and then stained with hematoxylin and eosin (H&E). Using the Olympus XC-10 microscope, the intratumoral, peritumoral, and tumoral areas were evaluated. Overall mice with GBM showed weight loss of ±28% mice with GBM injected in striatum showed severe kyphosis; meanwhile hippocampal GBM mice presented contralateral hemiparesia. Tumor growth gradually incremented the first three weeks and reached a peak at four weeks, showing an increase of 64%. The in vivo model of GBM in rodents can be used for future translational research approaches to prevent/ reduce the growth of glioblastoma.

Introduction

Treatment

Despite several advances in surgical and radiation techniques and new generation of chemotherapeutic drugs, GBM is the most invasive type of brain tumor.

Current therapies for GBM include radiotherapy/chemotherapy drugs (Temozolomide, etc.) and surgical removal.

Prognosis

The median survival rate of patients with GBM with treatment is only 12 to 16 months. The survival rate for patients without treatment is about 3 months.

Lack of early detection of GBM also contributes to the poor prognosis.

Seizure

Seizures are common in diffuse gliomas, occurring in 50–90% of low-grade astrocytoma patients and in 20–60% of glioblastoma patients. Seizures could be an initial symptom in 45 % of patients with GBM and often represent the first symptom of this deadly disease.

Objective:

To quantify xenotransplant growth of GBM cells into the brain of the mouse.

Methods and Materials

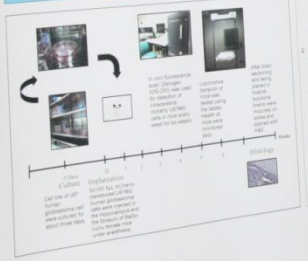

Results

Figure I: Striatum GBM

Figure II: Hippocampal GBM

Figure III: Histological Profile

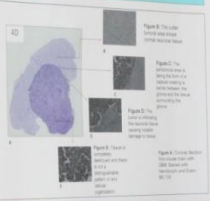

Conclusion

•Xenotransplants of GBM in brain grow progressively during six weeks, starting exponentially at four weeks

•Tumor growth impairs neurological functions expressed in locomotive activity

Acknowledgements

Special thanks to Om Prakash from S.S.C.C. L... S.S.C.C. Rachel Harris, summer student, and ... Lab Staff and Nicolas Bazan, Director of Neu...

6

Tulane University

Developing high-throughput zebrafish neurobehavioral screens for drugs of abuse

Jonathan Chawla, Jonathan Cachat, Sam Landsman, Michael Gebhardt, Mallorie Brimmer, Cassie Craddock, and Allan Kalueff
Tulane University School of Medicine – Department of Pharmacology,

LSU Health Sciences Center

Abstract

Methods

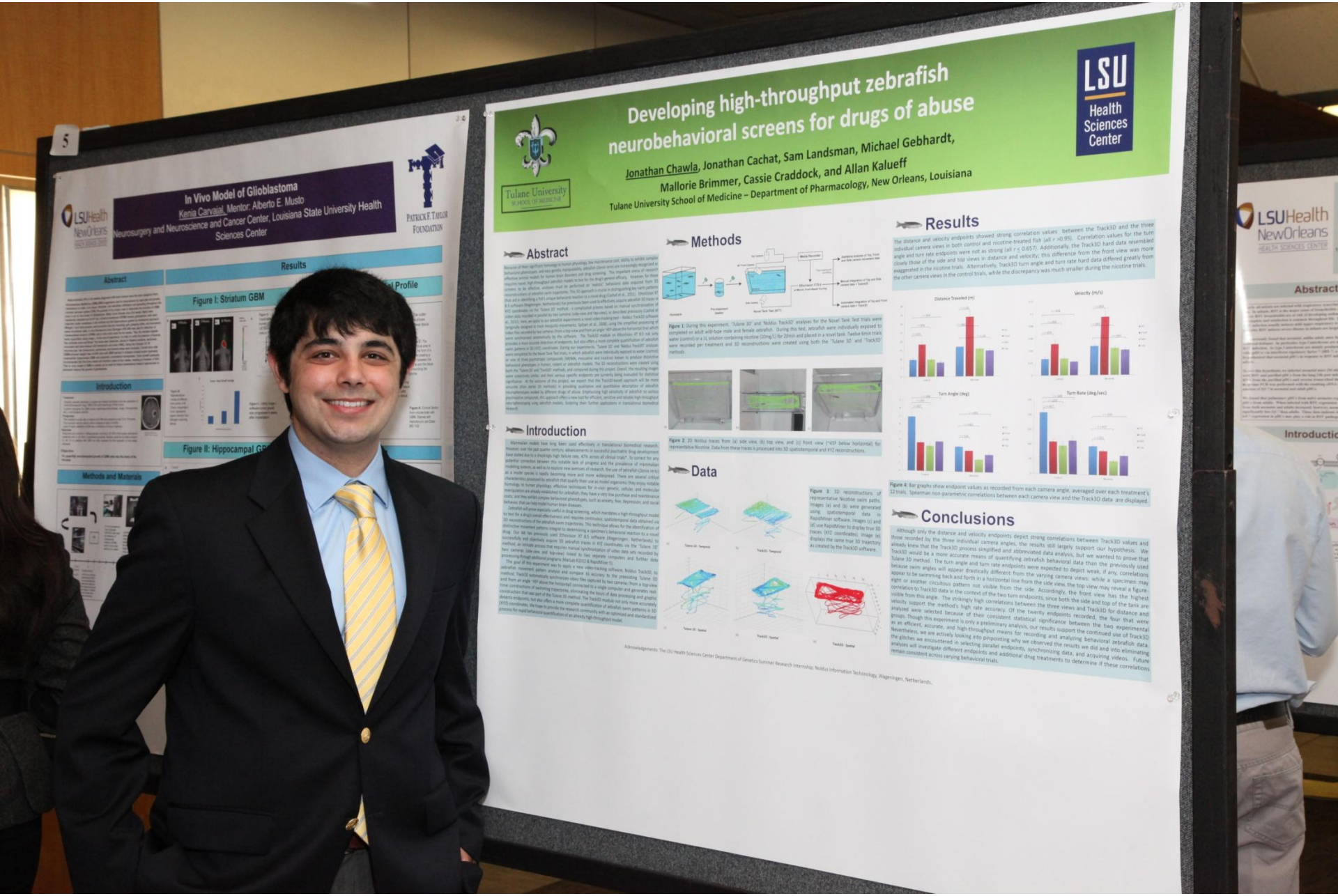
5
In Vivo Model of Glioblastoma
Kenia Carvalal, Mentor: Alberto E. Musto
Neurosurgery and Neuroscience and Cancer Center, Louisiana State University Health Sciences Center
Patrick F. Taylor Foundation
Abstract
Results
Figure I: Striatum GBM
Introduction
Figure II: Hippocampal GB
Methods and Materials
Developing high-throughput zebrafish neurobehavioral screens for drugs of abuse
Jonathan Chawla, Jonathan Cachat, Sam Landsman, Michael Gebhardt,
Mallorie Brimmer, Cassie Craddock, and Allan Kalueff
Tulane University School of Medicine – Department of Pharmacology, New Orleans, Louisiana
Tulane University School of Medicine
LSU Health Sciences Center
Abstract
Introduction
Methods
Figure 1: During this experiment, "Tulane 3D" and 'Noldus Track3D' analyses for the Novel Tank Test trials were completed on adult wild-type male and female zebrafish. During this test, zebrafish were individually exposed to water (control) or a 1L solution containing nicotine (10mg/L) for 20min and placed in a novel tank. Twelve 6min trials were recorded per treatment and 3D reconstructions were created using both the "Tulane 3D" and 'Track3D' methods.
Figure 2: 2D Noldus traces from (a) side view, (b) top view, and (c) front view (~45ºV below horizontal) for representative Nicotine. Data from these traces is processed into 3D spatiotemporal and XYZ reconstructions.
Data
Figure 3: 3D reconstructions of representative Nicotine swim paths. Images (a) and (b) were generated using spatiotemporal data in RapidMiner software. Images (c) and (d) use RapidMiner to display true 3D traces (XYZ coordinates). Image (e) displays the same true 3D trajectory as created by the Track3D software.
Results
Figure 4: Bar graphs show endpoint values as recorded from each camera angle, averaged over each treatment's 12 trials. Spearman non-parametric correlations between each camera view and the Track3D data are displayed.
Conclusions
Acknowledgements: The LSU Health Sciences Center Department of Genetics Summer Research Internship; Noldus Information Technology; Wageningen, Netherlands.

Allosteric regulation of Eg5 motility along microtubules

Victoria Dauphin[1], Rebecca Buckley[1], Thomas Huckaba[2], and Sunyoung Kim[1]

[1]Dept. Biochemistry, LSU School of Medicine & [2]Dept. Biology, Xavier University of Louisiana, New Orleans, LA

Abstract

Kinesin Eg5 is a motor protein that uses the energy derived from ATP hydrolysis to drive separation of spindle microtubules during metaphase of mitosis. When Eg5 function is inhibited cell division fails. Its essential role in mitosis makes it an attractive anti-cancer target. Over one hundred classes of inhibitors bind Eg5 at an allosteric hotspot known as the L5 loop. Despite extensive study on Eg5 inhibition, the normal role of L5, in the absence of inhibitors, remains unclear. During the catalytic cycle of Eg5, L5 undergoes conformational changes upon nucleotide and microtubule binding. Specifically, our lab has shown that residue substitutions within L5 alters ATP hydrolysis rates and loop conformation. However, the consequence of these changes on Eg5 motility along microtubules has not been studied. We hypothesize that L5 allosterically regulates Eg5 function and that Eg5 motility will be directly affected by substitutions in L5. We aim to test our hypothesis by performing microtubule (MT) gliding assays on L5 mutants to determine the rate of MT motility compared to wild type. This work will clarify how an allosteric site, L5, regulates the normal activity of the mitotic motor protein, Eg5.

Introduction

Human Eg5 kinesin is essential for formation of the metaphase spindle in mitosis. In its homotetrameric form, this motor protein slides antiparallel microtubules against each other.

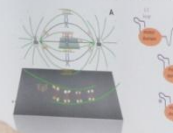

oop in the motor domain, termed L5, is necessary for kinesin function. This loop is not part of the nucleotide crotubule-binding site. How this L5 region of the protein unction is still not understood, but important to decipher ids candidate antimitotic drugs.

L5 loop substitutions affect ATPase activity of Eg5 kinesin.

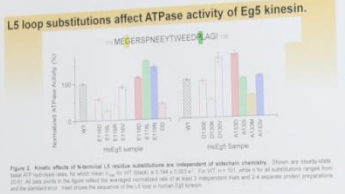

Figure 2. Kinetic effects of N-terminal L5 residue substitutions are independent of videochain chemistry. Shown are steady-state basal ATP hydrolysis rates for which mean k_{cat} for WT (black) ± 0.144 ± 0.003 s^{-1}. For MT, n = 101, while n for all substitutions ranges from 20-81. All data points in the figure reflect the averaged normalized rate (% of at least 3 independent trials and 2-4 separate protein preparations and the standard error. Inset shows the sequence of the L5 loop in human Eg5 kinesin.

Results

L5 loop substitutions affect microtubule motility driven by Eg5.

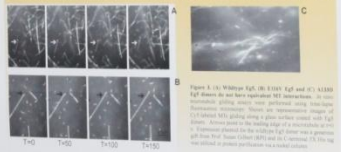

While the homotetramer is the cellular form of the protein, the kinesin dimer can walk along microtubules and give a functional readout of Eg5 activity.
The N-terminal substitution has a comparable motility rate to wildtype, but the C-terminal substitution blocks motility and organizes MTs into bundles.

Dimeric Eg5 kinesin can move single microtubules and also glide two antiparallel microtubules in opposite directions.

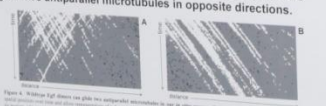

Figure 4. Wildtype Eg5 dimers can glide two antiparallel microtubules in our in vitro assays. Kymographs provide a graphical representation of space versus time and allow representation of a dynamic process on a single image. Here we useful in monitoring microtubules and characterizing its motion. (A) Homotetrameric kinesin is observed by the vertical stained lines crossing each other. (B) Single monodisperse monomers is observed by the vertical stained lines with no other microtubule crossing it.

Motility of wildtype Eg5 dimers were faster along antiparallel microtubules than single MTs.

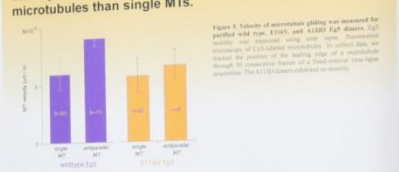

Figure 5. Velocity of microtubule gliding was measured for purified wild type, E116V, and A133D Eg5 dimers. Eg5 motility was measured using time lapse fluorescence microscopy of Cy5-labeled microtubules. To collect data, we tracked the position of the leading edge of a microtubule through 51 consecutive frames of a fixed-interval time-lapse acquisition. The A133D dimers exhibited no motility.

However, antiparallel MT motility for E116V Eg5 is similar to single MT motility.

Conclusions

Observed antiparallel MT gliding, in the presence of purified dimeric Eg5, reveals that a higher order oligomerization state of Eg5 must be formed in solution.

This implies that we have a form of the protein that can easily be purified and used as a tool to study the antiparallel gliding and bundling functions of the native tetrameric Eg5.

Our results also suggest that the native L5 loop is involved in long distance communication to the microtubule-binding site in the same motor domain.

We also conclude that alternations to the L5 loop may affect the coordination of motor domains with each other in the tetrameric kinesin complex.

Future studies will include single molecule tracking of Eg5 along MT.

Acknowledgments

We thank Prof. E. Wojcik for helpful discussions and his generous technical advice. This work is supported by NIH (GM097350 to S.K. 5G12RR026260 and 8P20GM103424-11 to T.H.), the Louisiana Cancer Research Consortium (T.H.), and the Dean of the LSU School of Medicine (V.D.).

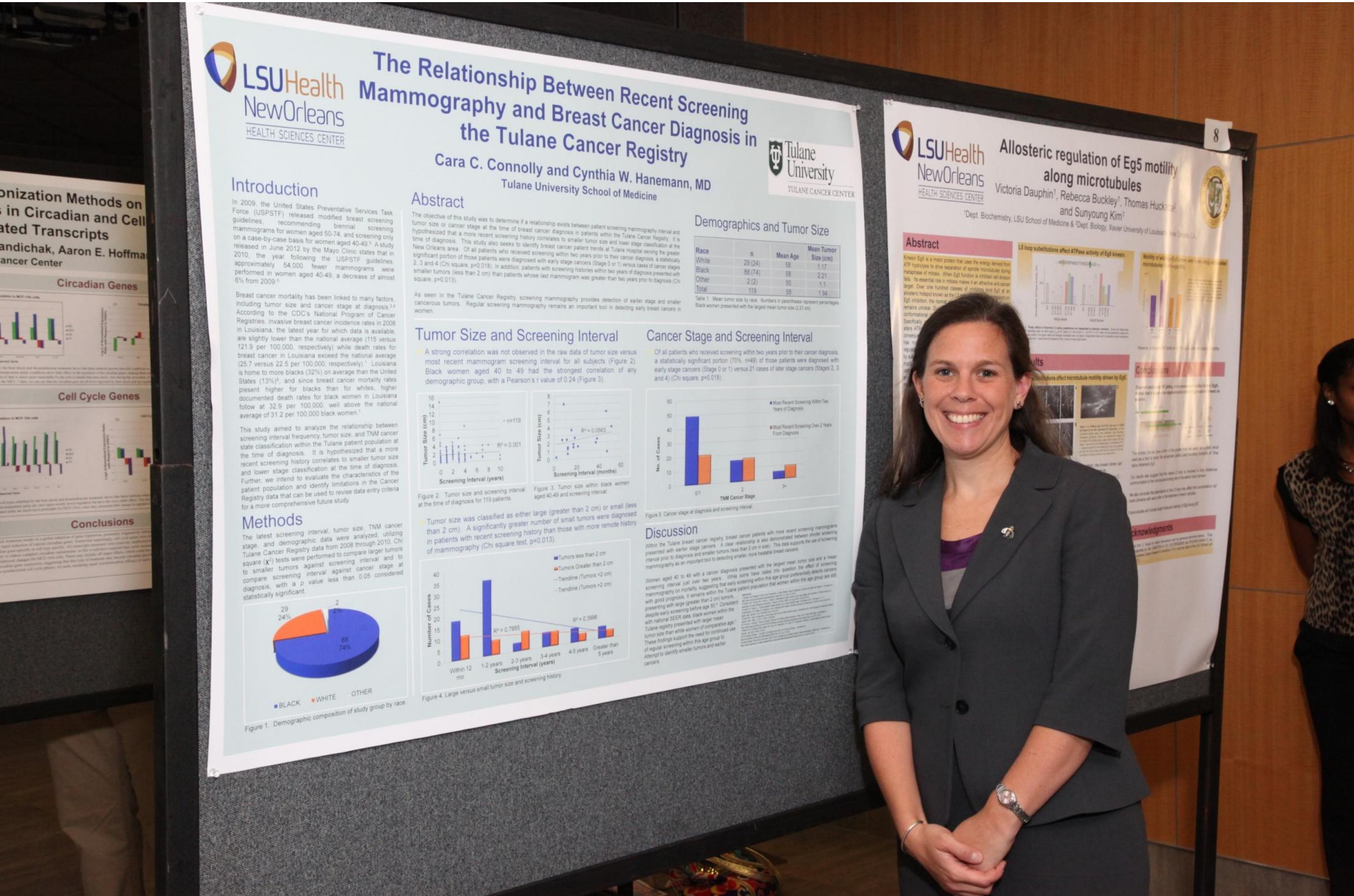
LSUHealth NewOrleans HEALTH SCIENCES CENTER
The Relationship Between Recent Screening Mammography and Breast Cancer Diagnosis in the Tulane Cancer Registry
Cara C. Connolly and Cynthia W. Hanemann, MD
Tulane University School of Medicine
Tulane University TULANE CANCER CENTER
Introduction
Abstract
Demographics and Tumor Size
Race n Mean Age Mean Tumor Size (cm)
White 29 (24) 58 1.17
Black 88 (74) 58 2.21
Other 2 (2) 50 1.1
Total 119 58 1.94
Tumor Size and Screening Interval
Cancer Stage and Screening Interval
Methods
Discussion
BLACK WHITE OTHER
Figure 1. Demographic composition of study group by race.
Figure 2. Tumor size and screening interval at the time of diagnosis for 119 patients.
Figure 3. Tumor size within black women aged 40-49 and screening interval.
Figure 4. Large versus small tumor size and screening history.
Figure 5. Cancer stage at diagnosis and screening interval.
LSUHealth NewOrleans HEALTH SCIENCES CENTER
Allosteric regulation of Eg5 motility along microtubules
Abstract
Conclusions
8
Circadian Genes
Cell Cycle Genes
Conclusions

Relevance of Prorenin Levels in the Urine of Patients with Diabetes

Gabrielle Dawkins
Department of Physiology, Tulane University School of Medicine, New Orleans, LA

LSUHealth NewOrleans HEALTH SCIENCES CENTER

Tulane University TULANE CANCER CENTER

Abstract

The effect of diabetes on intrarenal renin-angiotensin system (RAS) activity has been studied in animals and humans. The use of urinary angiotensinogen as a biomarker of intrarenal activation of the renin-angiotensin system (RAS) still remains controversial, mainly in diabetic patients, as its levels in urine are highly correlated with those of albuminuria. Diabetic patients suffering from microvascular complications exhibit high prorenin levels in plasma. The use of prorenin levels in urine as a potential early marker of these complications is of great interest due to recent demonstrations in animals that prorenin can be secreted by the collecting ducts during diabetes and hypertension. However, there has not been sufficient research relaying the effects of diabetes on urine levels of prorenin. The prevelue of this biomarker in urine reflects micro-vascular injury in these patients. We hypothesize that diabetic patients will have significantly higher levels of prorenin in the urine due to over activation of intrarenal RAS.

To test this hypothesis, we aimed to examine the effect of diabetes on prorenin levels in the urine. There were diabetic (N=72) and non-diabetic (N=180) patients that were grouped based on sex, race, BMI, estimated glomerular filtration rate (eGFR), and blood pressure. Enzyme-linked immunosorbent assay (ELISA) (Catalog #HPRENKTAP, Molecular Innovations, Novi, Michigan) was used to determine the concentrations of prorenin in the urine. These values were then corrected using urine creatinine values. These corrected values will be compared for each of the groups to examine the significance among the groups. We expect to demonstrate a significant correlation between urinary levels of prorenin and chronic kidney disease. If so, these data will indicate that the activation of intrarenal RAS, as reflected by the prorenin levels in the urine, could be used as a potential biomarker of CKD, thus used clinically to tailor therapeutic outcomes.

Introduction

Background

- Evidence indicates that intrarenal RAS regulation is independent of systemic RAS.
- In diabetes mellitus (DM), it has been shown that there is over activation of the intrarenal RAS in human and animal models.
- Diabetic patients exhibit high plasma prorenin levels which is associated with the severity of microvascular complications. However, in the urine, they have high renin levels.
- In diabetic rats, the major source of prorenin is the collecting duct.
- Previous studies have shown that during intrarenal RAS activation, such as in hypertension, there is augmentation of renin in the urine.

Aim

To determine if prorenin levels are augmented in the urine of diabetic patients in order to tailor therapeutic treatments in diabetic patients.

Hypothesis

Diabetic patients have significantly higher levels of prorenin in the urine due to over activation of intrarenal RAS.

Materials and Methods

This study consisted of urine samples from 72 diabetic patients and 180 non-diabetic patients. The urine samples were concentrated 10X using Millipore filters (Catalog #UFC9100, EMD Millipore, Billerica, MA). ELISA (Catalog #HPRENKTAP, Molecular Innovations, Novi, Michigan) that was specific for Prorenin was used. Using spectrophotometry, the concentration of prorenin in each sample was calculated in ng/mL. These prorenin concentrations were then corrected by using urine creatinine concentrations. Each sample is measured in ng of prorenin per gram of creatinine.

Demographic Characteristics

Variables	Diabetic (n=72)	Non-Diabetic (n=180)	P-value for difference
Age, in years	55.44 ± 1.117	42.16 ± 1.055	<0.0001****
Body Mass Index, kg/m2	36.63 ± 0.7793	29.38 ± 0.5995	<0.0001****
African American, %	61.11	38.89	0.0072**
Female, %	65.28	60	0.4165
Systolic Blood Pressure, mmHg	128.6 ± 3.104	121.3 ± 1.275	0.0095**
Diastolic Blood Pressure, mmHg	82.04 ± 2.026	75.63 ± 0.8419	0.0015**
eGFR, mL/min	68.34 ± 1.970	70.15 ± 0.5362	0.2288
Prorenin to Creatinine ratio, ng/g	263.4 ± 36.07	65.34 ± 13.69	<0.0001****
N/A			

Log Transformations

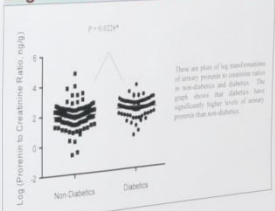

These are plots of log transformations of urinary prorenin to creatinine ratios in non-diabetics and diabetics. The graph shows that diabetics have significantly higher levels of urinary prorenin than non-diabetics.

Results

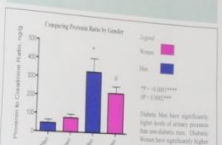

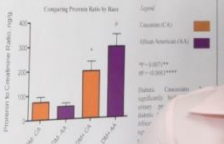

Conclusion

There is a significant difference in urinary prorenin lev
patients. There is no significant difference in urinary pr
between Caucasians and African Americans. Therefore
used as a measure of over activation of intrarenal
medications and therapeutic efforts can then be
these patients.

Expression of *Irf-7* in Plasmacytoid Dendritic Cells is Limited Following Neonatal Respiratory Syncytial Virus Infection

Joshua Daye[1,2], Dahui You [1], and Stephania Cormier [1]

[1]Department of Pharmacology and Experimental Therapeutics, Louisiana State University Health Sciences Center, New Orleans, Louisiana, USA

[2]Dillard University, New Orleans, Louisiana, USA

LSU Health New Orleans Health Sciences Center

Louisiana Vaccine Center

Abstract

Nearly all infants are infected with respiratory syncytial virus (RSV) by two years of age. In infants, RSV is the major cause of bronchiolitis and infants who acquire severe RSV bronchiolitis are at risk of developing asthma. Immune protection is incomplete and reinfection is common throughout life. In otherwise healthy adults, RSV infection usually induces mild upper respiratory tract disease. The mechanisms whereby RSV induces severe disease in infants are largely unknown.

We previously found that neonatal, unlike adult, mice fail to induce appropriate anti-viral defenses. In particular, type I interferons are not produced in response to RSV infection. As type I interferons are mainly produced by plasmacytoid dendritic cells (pDCs) via interferon regulatory factor 7 (IRF-7; a transcription factor), we hypothesized that neonatal pDCs in response to RSV infection express less *Irf-7* than adults.

To test this hypothesis, we infected neonatal mice (5d old) and adult mice (7-8wks old) with RSV and purified pDCs from the lung 24h post infection. We then isolated total RNA from the purified pDCs and reverse transcribed the RNA to produce cDNA. Real-time PCR was performed with the resulting cDNA to quantify the relative amount of *Irf-7* in neonatal and adult pDCs.

We found that pulmonary pDCs from naïve neonates express seven fold less *Irf-7* than pDCs from adults. When infected with RSV, expression of *Irf-7* in pulmonary pDCs from both neonates and adults increased; however, neonatal pDCs expressed significantly less *Irf-7* than adults. These data indicate that the muted induction of Irf-7 expression in pDCs may play a role in RSV pathogenesis in neonates.

Introduction

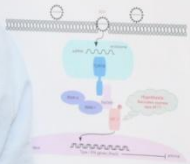

pe I IFN production in adult pDCs. RSV enters the cells and ovirus releasing its genomic ssRNA. ssRNA is recognized by host ade of signaling events leading to the phosphorylation of IRF-7. translocates to the nucleus and promotes the expression of type I IFNs.

Methods

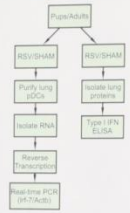

Fig 2: Schematic of the experimental design. Five day old pups or 6-8 wks old adults were infected with RSV or sham infected with media. At one day post infection, total protein was isolated from the lungs of half of the mice. Type I IFNs were measured in the isolated protein using ELISA. The other half of the mice were used for lung pDC purification. RNA were isolated from these purified pDCs and reverse transcribed to cDNA. The resulting cDNA were subjected to real-time PCR to measure the expression of *Irf-7* in pDCs.

Purity of the Isolated pDCs

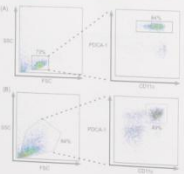

Fig 3: Purity of the isolated pDCs. Five day old pups and 6-8 wks old adults were infected with RSV. The pDCs were purified using gradient density centrifugation and magnetic bead selection. The resulting cells from the purification were then labeled with CD11c and PDCA-1 antibodies to identify pDCs. (A) Purified pDCs from adult lung. (B) Purified pDCs from neonatal lung.

Neonatal RSV Infection Induced Limited Expression of *Irf-7*

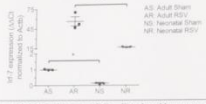

Fig 4: Relative expression of *Irf-7* in pulmonary pDCs. Five day old neonates or 6-8 wks old adults were infected with RSV. pDCs were purified at 1 day post infection; and the expression of *Irf-7* in these cells were quantified using real time PCR. NS: sham infected neonates; NR: RSV infected neonates; AS: sham infected adults; AR: RSV infected adults. *: p<0.05.

Neonatal RSV Infection Induced Limited Type I IFNs Response

	IFNα (ng/g lung protein)	IFNβ (ng/g lung protein)
NS	4.35 ± 0.78	5.57 ± 1.13
AS	3.77± 0.89	8.14 ± 2.31
NR	5.51± 1.02	11.8 ± 2.43*
AR	76.2 ± 11.2*#	42.3 ± 5.07*#

Fig 5: Type I IFNs in lung homogenates. Neonatal or adult mice were infected with RSV and total lung protein was isolated using T-Per (Pierce). IFNα and IFNβ were then measured using ELISA at 1 day post-infection. NS: sham infected neonates; NR: RSV infected neonates; AS: sham infected adults; AR: RSV infected adults. *: p<0.05; NR vs. NS or AR vs. AS; #: AR vs. NR.

Conclusions

- Neonatal pDCs express less *Irf-7* than adult pDCs at baseline.
- RSV infection induces *Irf-7* expression in both neonatal and adult pDCs; however, expression of *Irf-7* in pDCs from neonates is muted compared to adults.
- RSV infection induces limited amount of type I IFNs (IFNα and β) in neonates.
- The muted expression of *Irf-7* and resulting reduction in type I IFNs may play a role in neonatal RSV pathogenesis.

Acknowledgement

The project described was supported by LVC and Grant Number (5R01 AI090059) from NIAID. Its contents are solely the responsibility of the authors and do not necessarily represent the official views of NIAID/NIH.

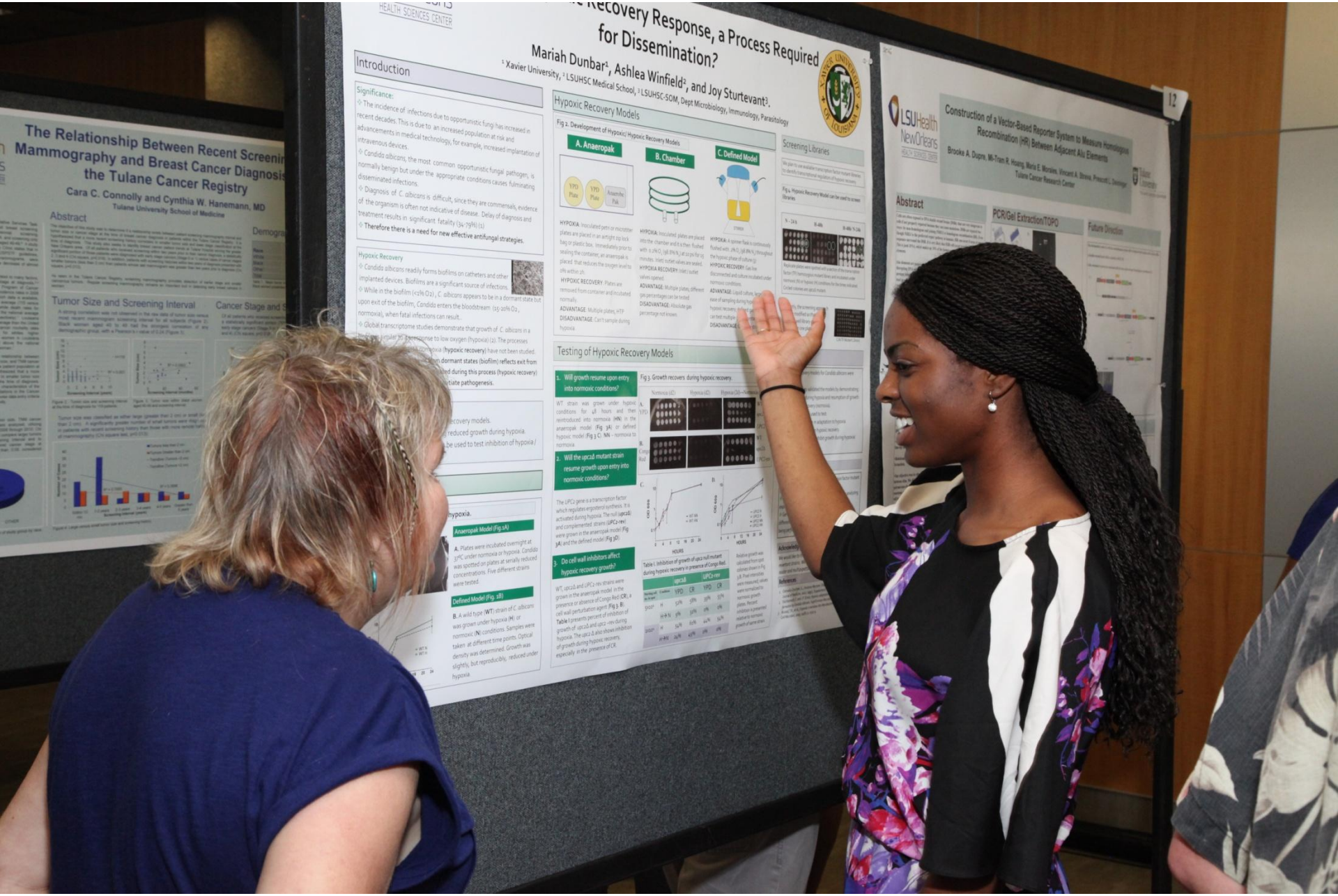
The Relationship Between Recent Screenin
Mammography and Breast Cancer Diagnosis
the Tulane Cancer Registry
Cara C. Connolly and Cynthia W. Hanemann, MD
Tulane University School of Medicine
Abstract
Tumor Size and Screening Interval
Cancer Stage and
Recovery Response, a Process Required
for Dissemination?
Mariah Dunbar[1], Ashlea Winfield[2], and Joy Sturtevant[3].
[1] Xavier University, [2] LSUHSC Medical School, [3] LSUHSC-SOM, Dept Microbiology, Immunology, Parasitology
Introduction
Significance:
Hypoxic Recovery
Hypoxic Recovery Models
A. Anaeropak
B. Chamber
C. Defined Model
Testing of Hypoxic Recovery Models
Anaeropak Model (Fig 1A)
Defined Model (Fig. 1B)
Construction of a Vector-Based Reporter System to Measure Homologous
Recombination (HR) Between Adjacent Alu Elements
Brooke A. Dupre, Mi-Tram R. Hoang, Maria E. Morales, Vincent A. Brove, Prescott L. Deininger
Tulane Cancer Research Center
Abstract
PCR/Gel Extraction/TOPO
Future Direction
12

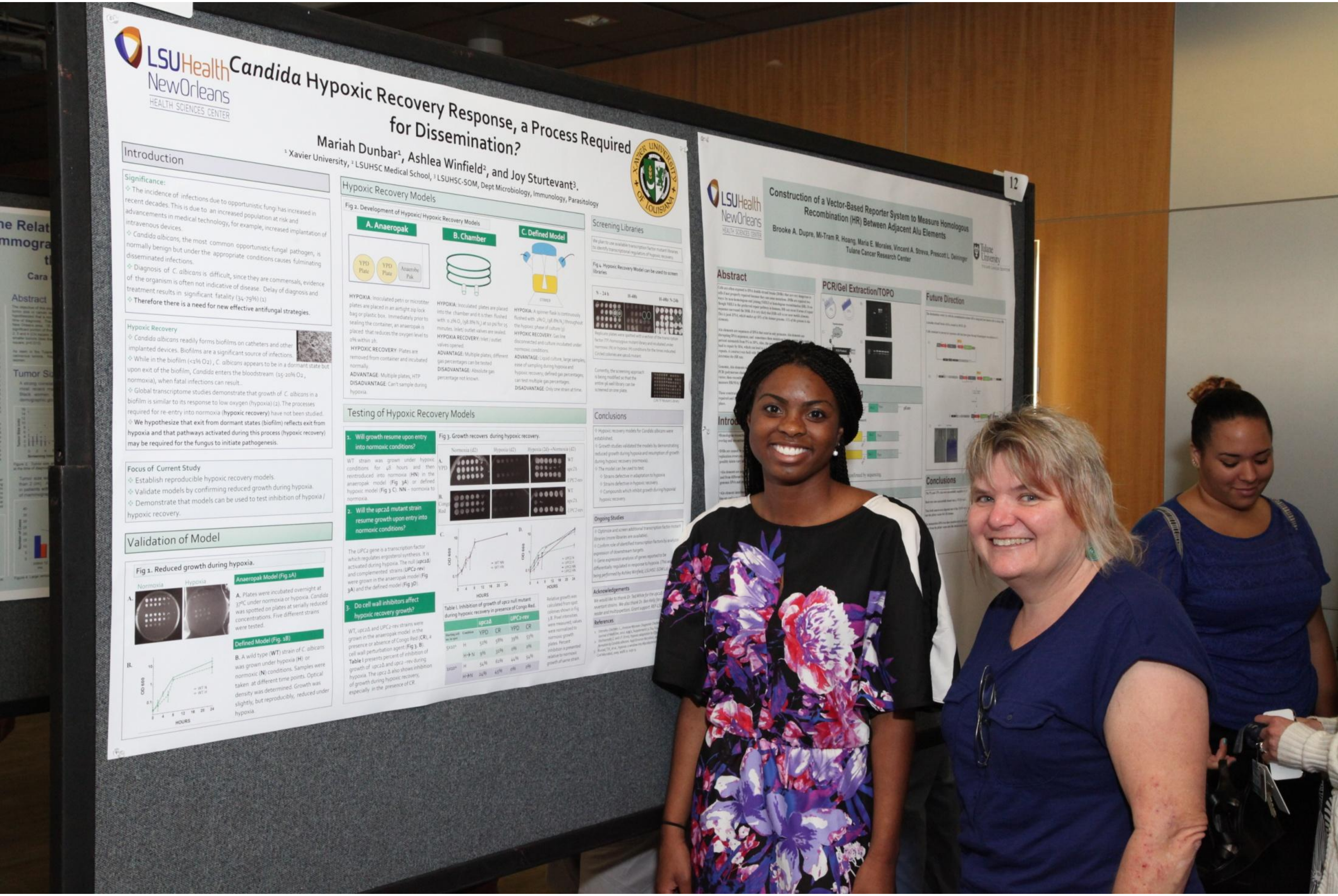
LSUHealth NewOrleans
HEALTH SCIENCES CENTER
Candida Hypoxic Recovery Response, a Process Required for Dissemination?
Mariah Dunbar¹, Ashlea Winfield², and Joy Sturtevant³.
¹ Xavier University, ² LSUHSC Medical School, ³ LSUHSC-SOM, Dept Microbiology, Immunology, Parasitology
XAVIER UNIVERSITY OF LOUISIANA
Introduction
Significance:
Therefore there is a need for new effective antifungal strategies.
Hypoxic Recovery
Focus of Current Study
Establish reproducible hypoxic recovery models.
Validate models by confirming reduced growth during hypoxia.
Demonstrate that models can be used to test inhibition of hypoxia / hypoxic recovery.
Validation of Model
Fig 1. Reduced growth during hypoxia.
Anaeropak Model (Fig.1A)
Defined Model (Fig. 1B)
Hypoxic Recovery Models
Fig 2. Development of Hypoxic/ Hypoxic Recovery Models
A. Anaeropak
B. Chamber
C. Defined Model
Testing of Hypoxic Recovery Models
1. Will growth resume upon entry into normoxic conditions?
2. Will the upc2Δ mutant strain resume growth upon entry into normoxic conditions?
3. Do cell wall inhibitors affect hypoxic recovery growth?
Fig 3. Growth recovers during hypoxic recovery.
Screening Libraries
Conclusions
Ongoing Studies
Acknowledgements
References
12
LSUHealth NewOrleans
HEALTH SCIENCES CENTER
Construction of a Vector-Based Reporter System to Measure Homologous Recombination (HR) Between Adjacent Alu Elements
Brooke A. Dupre, Mi-Tram R. Hoang, Maria E. Morales, Vincent A. Streva, Prescott L. Deininger
Tulane Cancer Research Center
Tulane University
Abstract
PCR/Gel Extraction/TOPO
Future Direction
Conclusions

11

Candida Hypoxic Recovery Response, a Process Required for Dissemination?

Mariah Dunbar[1], Ashlea Winfield[2], and Joy Sturtevant[3].
[1] Xavier University, [2] LSUHSC Medical School, [3] LSUHSC-SOM, Dept Microbiology, Immunology, Parasitology

Introduction

Hypoxic Recovery Models

Screening Libraries

Testing of Hypoxic Recovery Models

Validation of Model

Construction of a Vector-Based Reporter System to Measure Homologous Recombination (HR) Between Adjacent Alu Elements

Brooke A. Dupre, Mi-Tram R. Hoang, Maria E. Morales, Vincent A. Streva, Prescott L. Deininger
Tulane Cancer Research Center

Tulane University
TULANE CANCER CENTER

Abstract

Cells are often exposed to DNA double strand breaks (DSBs) that are very dangerous to cells if not properly repaired because they can cause mutations. DSBs are repaired two ways by non-homologous end joining (NHEJ) or homologous recombination (HR). Even though NHEJ is the preferred repair pathway in humans, HR can occur if areas of repeat sequence surround the DSB. It is very likely that DSBs will occur near mobile elements. This is true DNA, which makes up 50% of the human genome. 11% of the genome is Alu elements.

Alu elements are sequences of DNA that exist in only primates. Alu elements can disrupting DNA sequences, and sometimes these mutations lead to cancer. Alus range in percent mismatch from 5% to 30%. Also, the presence of Alu elements around a DSB can lead to repair by SSA, which can lead to a deletion of the DNA between the two Alu repeats. A construct was built with 5% and 15% mismatches between Alu elements to determine the HR rate.

Genomic Alu elements with 5% and 15% of mismatched base-pairs were amplified by PCR (polymerase chain reaction). The PCR products were then subcloned into an Entry vector, then recombined into a destination vector (constructed in the Deininger lab to measure HR/SSA) by LR clonase, part of the gateway system.

These constructs will be inserted into mammalian cells to observe how the DSBs are repaired and if the different percentages of mismatch DNA affect which process takes place.

Introduction

•Homologous recombination is when two ends of a DNA double stranded break (DSB) overlap and recombine. The DNA is exchanged and a deletion occurs.

•DSBs are caused by several different factors such as: radiation, thermal disruption, replication errors etc. DSBs can be very dangerous if not repaired correctly because they can possibly delete very important segments of DNA.

•Alu elements are sequences of DNA that exist solely to replicate themselves and relocate to and from different loci in the genome. They make-up approximately 11% of all human genomic DNA and are usually found in 300 basepair sequences.

•Alu element interference sometimes can cause deletion after a DSBs because the Alus will line-up and sometimes delete nucleotides between the break and where they line-up.

•Deletion may end in cancer if a deletion occurs that causes over reproduction and tumor formation.

•Our objective was to observe if the percentage or amount of mismatched DNA affected HR between Alus. We did this by amplifying 5% and 15% mismatched Alu DNA through a polymerase chain reaction (PCR). The PCR product was then used in a series of cloning reactions to obtain our mismatched Alu elements in a recombination reporter cassette which will later be used to test HR in human cells.

PCR/Gel Extraction/TOPO

pEntr Cloning

LR Recombination

Future Direction

The destination vector (A) with the recombination system will be integrated into human cells in culture (B).

A double strand break will be created by ISCE1 (B)

Cells resistant to puromycin represent cells that have gone through Homologous recombination (C)

Conclusions

The 5% and 15% Alu were successfully amplified by PCR

Both were also successfully cloned into a TOPO vector

Then both inserts were digested out of the TOPO with restriction enzymes and then they were subcloned into the pEntr vector for LR clonase.

The mismatched DNA was then transferred to the destination vector using LR clonase to exchange the insert from the pEntr vector into the destination vector.

LSUHealth NewOrleans HEALTH SCIENCES CENTER

Influenza Vaccination Program Requirements of Healthcare Personnel in Louisiana Hospitals

Kayla Fricke, Mariella Gastañaduy, Renee Kloss, Rodolfo Bégué
LSUHSC-NOLA, Department of Pediatrics, Division of Infectious Diseases and Children's Hospital, New Orleans

LVC Louisiana Vaccine Center

Introduction

- Influenza virus causes 24,000 annual deaths in the U.S. Every year 450,000 to 900,000 Louisiana residents are infected and 800 die.
- To prevent high morbidity and mortality, annual vaccination of patients and healthcare personnel (HCP) is recommended. Yet, the vaccination coverage of U.S. HCP in 2010 was only 60%.
- In response, the Centers for Disease Control and Prevention (CDC) is demanding that vaccination rates improve to 90% by 2020, and various Medical Societies are recommending mandatory vaccination programs (i.e., requirement for employment).
- To improve influenza vaccination coverage of HCP in Louisiana hospitals we must first understand what is being done, what is effective and what is ineffective.

Objectives

1. To determine influenza vaccination requirements and policies among hospitals in Louisiana, including the prevalence of mandatory requirements and consequences for declination
2. To correlate specific requirements with vaccination rates achieved, and to identify interventions that may increase vaccination rates

Methods

- A survey was sent to all 256 hospitals in Louisiana (under 193 organizations) identified in the Directory of the Louisiana Hospital Association.
- The survey contained questions on type of hospital, patient population served, components of the vaccination program and their estimated vaccination rate.
- Data was inputted into an Excel sheet and analyzed for components that influenced vaccination rates.
- Univariant analysis of categorical data compared the median vaccination rate between hospitals with or without a specific variable using the non-parametric Mann-Whitney test.
- The effect of continuous variables on the vaccination rate was analyzed with regression analysis using the non-parametric Spearman r.
- A p Value of <0.05 was considered significant.

Results: Hospitals Responding

- In the first 4 weeks, 49 (25%) of the 193 administrations responded with a statewide distribution (Figure 1).

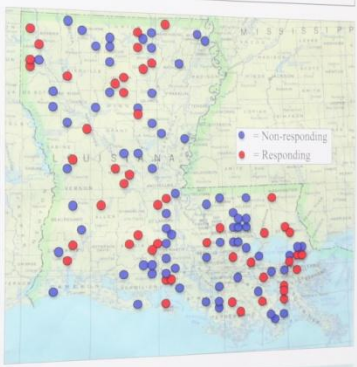

Results: Main Responses

- Most hospitals were private for profit (51%); private non-profit (35%), and public (14%); 22% were teaching and 51% were accredited by The Joint Commission.
- The median number of beds was 60 with a range of 10 – 800.
- All hospitals had a flu vaccination program; 33% had voluntary vaccination and 67% required a formal declination. No hospital demanded vaccination as a requirement of employment.
- All hospitals offered free vaccines; 27% met all CDC recommended activities for vaccination but 73% did not meet all CDC recommendations.
- 24% of hospitals enforced consequences to HCP declining vaccination while 76% had no consequences; the most common consequence was a requirement to wear a mask on patient contact.
- The median vaccination rate reported by the responding hospitals was 61%, with a range from 12 - 98%.

Results: Correlates of Vaccination

Factors Positively Associated with Vaccination Rates

Survey Questions	No. Responses	%	Not Present	Present	Ratio	p Value
			Median (25%, 75%)			
Hospital Type						
Private	18	37	55 (45, 72)	73 (58, 84)	1.33	0.02
Acute Care	28	58	50 (45, 72)	70 (57, 83)	1.40	0.02
High-Risk Patient Type						
Children	29	59	50 (45, 71)	70 (56, 83)	1.40	0.02
Pregnant Women	23	47	51 (45, 71)	72 (60, 83)	1.41	0.004
Intensive Care	26	53	50 (42, 70)	71 (57, 85)	1.42	0.006
Number of Beds						
0 - 99	26	53		50 (45, 71)	0.694	0.0006
100 - 299	12	24		70 (56, 80)	1.186	
≥ 300	8	16		85 (61, 92)	1.464	
Vaccination Program						
Voluntary	16	33	71 (52, 85)	52 (40, 67)	0.73	0.001
Declination Required	33	67	52 (40, 67)	71 (52, 85)	1.37	0.001
Vaccine Administration						
Common areas	31	63	48 (37, 52)	70 (59, 83)	1.46	0.001
Nights/Weekends	18	78	50 (35, 62)	70 (53, 84)	1.40	0.004
Program Promotions						
Fliers	37	76	43 (33, 56)	69 (53, 80)	1.60	0.005
Email	34	69	50 (45, 71)	66 (54, 84)	1.32	0.05
Consequences upon Declination						
None	37	76	86 (82, 93)	55 (45, 70)	0.64	0.0001
Some consequence	12	24	55 (45, 70)	86 (82, 93)	1.56	0.0001
Wear mask	12	20	56 (44, 70)	89 (85, 94)	1.59	0.0001

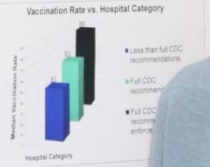

Conclusions

- Preliminary results demonstrate large variability among programs in Louisiana hospitals. No hospital required condition of employment.
- Hospitals that impose consequences for vaccine decli vaccination rate than hospitals without consequences
- Our findings suggest that to reach the goal of 90% va programs with consequences for declination (e.g. wea enforced.
- These findings have important public health implicat

LSUHealth NewOrleans HEALTH SCIENCES CENTER

Optimization: Dose, Timing, and Route of BMSCs to Improve Quality of Life and Life Span in Mice with Krabbe's Disease

Peter Gold, Brittni Scruggs, Dr. Bruce Bunnell
Center for Stem Cell Research and Regenerative Medicine, Tulane University School of Medicine

Krabbe's Disease

Motor Function Testing

IP

ICV

TUNEL Assay: Detection

Histological Staining – Infiltrating cells

Post Cell-Therapy Enzy

Conclusions

Optimization: Dose, Timing, and Route of BMSCs to Improve Quality of Life and Life Span in Mice with Krabbe's Disease

Peter Gold, Brittni Scruggs, Dr. Bruce Bunnell
Center for Stem Cell Research and Regenerative Medicine, Tulane University School of Medicine

LSUHealth NewOrleans HEALTH SCIENCES CENTER

Tulane University TULANE CANCER CENTER

Krabbe's Disease

- Krabbe's Disease, also known as globoid cell leukodystrophy (GLD), is an autosomal recessive disease affecting both the central and peripheral nervous systems' white matter caused by a deficiency of galactosylceramidase enzyme (GALC).
- GALC is a lysosomal enzyme that is responsible for metabolism of glycolipids such as galactosylceramide (GalCer) and galactosphingosine (psychosine) during active myelination.
- Inability to breakdown these glycolipids causes psychosine buildup, leading to pathological features of Krabbe's Disease: apoptosis in the brain, extensive inflammation of blood vessels in both nervous systems, axonal loss and demyelination of neurons.
- Krabbe's Disease shows onset of symptoms (e.g., seizures, irritability, vomiting, fever, mental and development delay) between ages 4-6 months, and is often fatal in infants before 2 years. There is no cure for Krabbe's Disease.
- Twitcher mice are an authentic model of human Krabbe's Disease that developed through spontaneous mutation of the GALC gene (GALC^{twi}).

Multipotent Stromal Cells (MSCs)

- BMSCs are known to express GALC, modulate immune reactions in vitro, and at the same time do not create an immunological response in vivo. They can be harvested and expanded easily in culture for clinical setting use.
- Their abilities include: self-renewal and differentiation in numerous categories of cell types. They are exceptional candidates for restoration of damaged tissue.
- BMSCs have been known to promote cellular proliferation within the brain, secrete a variety of cytokines and growth factors that have paracrine activities, and promote differentiation of the host's stem cells.
- BMSC treatment may be a safer option for Krabbe's Disease treatment over the current BMT treatment because of suppression of T-lymphocyte proliferation by allogeneic BMSCs. BMT often leads to the development of Graft Versus Host Disease (GVHD).

Treatment Groups and Goals

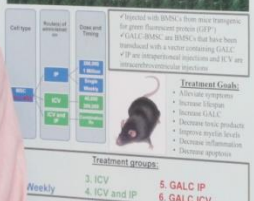

- Injected with BMSCs from mice transgenic for green fluorescent protein (GFP+)
- GALC-BMSC are BMSCs that have been transduced with a vector containing GALC
- IP are intraperitoneal injections and ICV are intraventricular injections

Treatment Goals:
- Alleviate symptoms
- Increase Lifespan
- Increase GALC
- Decrease toxic products
- Improve myelin levels
- Decrease inflammation
- Decrease apoptosis

Motor Function Testing

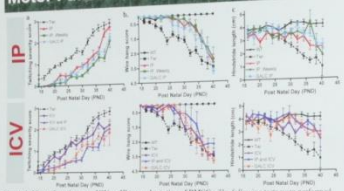

Figure 1. Motor function post ICV or IP transplantation of BMSCs. The following tests were performed for wild type (WT; N=17), non-injected twitcher mice (Twi; N=26), ICV-treated twitcher mice (200,000 BMSCs) (ICV; N=7), GALC ICV-treated twitcher mice (GALC ICV; N=6), combination ICV and IP-treated twitcher mice (ICV and IP; N=5), IP-treated twitcher mice (1 million BMSCs) (IP; N=18), IP weekly-treated twitcher mice (IP Weekly; N=8), and GALC IP-treated twitcher mice (GALC IP; N=9) starting at post-natal day (PND) 14. All mice were monitored daily and euthanized at 20% of the maximum body weight or when they become moribund. (a) Twitching severity was assessed for all twitcher mice. (b) Hind-leg strength was assessed using the wire hang test. (c) Hindstride was measured for assessment of gait.

Histological Staining – Infiltrating cells

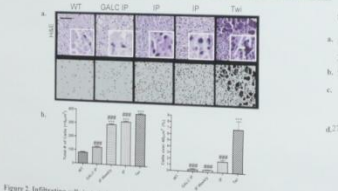

Figure 2. Infiltrating cells in twitcher sciatic nerve (a) Sciatic nerves from wild type, GALC IP-treated, IP weekly-treated, IP-treated (1 million BMSCs), and untreated twitcher mice were obtained after euthanasia at PND37 and processed using Hematoxylin and Eosin (HE) stains. The scale bar represents 50 microns for all larger images (10x), and each smaller image (40x) is a four-fold magnification of the larger image. (b) The number of infiltrating immune cells in the HE stains of GALC IP-treated twitchers (GALC IP, N=3), IP weekly-treated twitchers (IP Weekly, N=4), IP-treated twitchers (IP, N=4)) and non-injected twitcher (Twi, N=4) groups were calculated, compared to the total pixels for each scanned image, and normalized to the WT group (N=5). Comparisons were made using one-way ANOVA and Bonferroni's post-hoc testing, where *** P<0.001 vs. WT and ### P<0.001 vs. Twi.

TUNEL Assay: Detection of Apoptosis

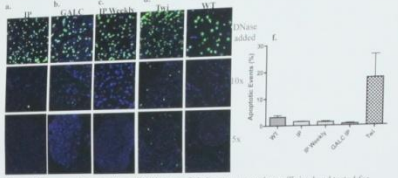

Figure 3. Fluorescent images after TUNEL Assay. Sciatic nerves were deparaffinized and tested for apoptotic events (green) using an *in situ* cell death fluorescein detection kit (Roche Diagnostics); all sciatic nerves were imaged at 5x and 10x magnification after dapi (blue) nuclear staining. For each nerve tested, a positive control was performed using DNase to test efficiency of the TUNEL Assay. Sciatic nerves were tested for the following treatment groups: (a) IP-treated twitcher (IP), (b) GALC IP-treated twitcher (GALC), (c) IP-treated weekly twitcher (IP weekly), (d) Untreated Twitcher (Twi), and (e) Wild Type (WT). (f) Quantification of apoptotic events was assessed using Image J analysis.

Post Cell-Therapy Enzyme Assessment

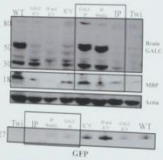

Figure 4. Western Blot for GALC, MBP, and GFP protein levels in the brain. Wild Type (WT), GALC ICV-treated twitcher (GALC ICV), combination IP and ICV-treated twitcher (IP and ICV), ICV-treated twitcher (ICV), GALC IP-treated twitcher (GALC IP), IP-treated weekly twitcher (IP Weekly), IP-treated twitcher (IP), and non-injection twitcher (Twi) brain samples were tested by western blot, and each lane represents the brain lysates of three mice pooled for protein analysis. (a) Bands present at 30 and 50 kDa denoted active GALC enzyme, (b) myelin basic protein (MBP), shown as a band at 18 kDa, indicated the presence of myelin, (c) actin protein was detected at 42kDa for each sample, and (d) green fluorescent protein (GFP) was detected as a band at 27kDa. An increase in GALC or MBP in any treatment group compared to the untreated group indicated improved lysosomal enzyme or myelin levels, respectively, in the brain after cell-therapy, whereas a band for GFP indicated that the administered GFP$^+$ cells were present in the mouse brain at the time of euthanasia.

Conclusions

- IP injections of eGFP$^+$ BMSCs improved hind leg strength and the severity of twitching compared to non-injection and ICV-BMSC injected mice. Significant improvements in motor function and twitching severity were achieved by further increasing the number of injections from single to weekly IP BMSC administration.
- Molecular studies support the findings that IP injections improve the pathophysiology of the twitcher mouse by decreasing inflammation and apoptosis in peripheral nerves, decreasing pro-inflammatory cytokine levels in kidney, increasing brain GALC levels and improving brain pathology.
- Molecular preliminary data show ICV injections decrease pro-inflammatory cytokine levels in the brain, and decrease globoid cell formation.
- Any clinical improvement resulting from MSC transplantation in the murine or primate models of Krabbe's Disease would indicate a promising future for such cells as a novel therapeutic for patients affected with globoid cell leukodystrophy or other glycosphingolipid storage disease.

LSUHealth NewOrleans HEALTH SCIENCES CENTER

Candida Invasion of Endothelial Cells Disrupts Intercellular Adhesion and VEGF Signaling

[1] Ciara Green and [2] Doug Johnston, PhD
[1] Southern University at New Orleans, [2] LSU Health Sciences Center

LVC Louisiana Vaccine Center

Abstract

Candida species are common commensal fungi found colonizing the oral, gastrointestinal tract, and ano- genital regions of humans. However, in immunocompromised patients the overgrowth of these fungi can lead to infections ranging from mild or superficial infections (e.g. thrush, vaginitis, etc.) to potentially fatal candidemia (fungi in the bloodstream). Some common contributing factors leading to candidiasis include: over use of stimulants (alcohol and drugs), underlying illness, surgery, diabetes, pregnancy, frequent antibiotic usage, malnutrition, and stress. Current antifungal therapies are insufficient as the medications tend to be expensive and/or toxic and there is an increasing prevalence of resistant organisms.

Candidemia associated with septic shock accounts for a large percentage of deaths among patients in intensive care settings. Previous findings in our lab have shown that the endothelial cells lining the blood vessels respond to *Candida* invasion by increasing expression of several genes involved with vascular repair and inflammation. The aim of this study was to determine the endothelial response with regard to the maintenance of vascular integrity, particularly those genes involved with cell-cell adhesion and cell signaling. We used a model of endothelial-*Candida* co-culture to identify changes in endothelial gene expression. Quantitative RT-PCR results showed increased expression of vascular endothelial growth factor (VEGF) mRNA, a primary regulator of endothelial proliferation, migration, and differentiation. Interestingly, we find no evidence of VEGF protein expression. As we also find decreased VEGF signaling in the presence of *Candida*, we used qRT-PCR and ELISA to study changes in endothelial signaling components. Our data indicate increased expression of a secreted version of VEGF receptor 1 VEGFR1 (sFlt-1), considered to be a negative regulator of VEGF signaling. Immunofluorescent data show that *Candida* induces rapid dissolution of VE-Cadherin junctions between neighboring cells and disruption of actin filaments resulting in the formation of large intercellular gaps. Further studies using immunoprecipitation, SDS-PAGE and Western Blotting revealed association of VE-Cadherin with both VEGFR1 & VEGFR2, and may contribute to the inhibition of VEGF responses. Collectively, our results show that *Candida* invasion of endothelium induces changes in cell-cell junctions and intracellular signaling that likely contribute to vascular dysfunction leading to symptoms of septic shock.

Introduction

The aim of this study was to determine the endothelial response to invasion by *Candida spp*, particularly those genes involved with cell-cell adhesion and VEGF signaling. Endothelial cells line the blood vessels and are responsible for maintaining vascular integrity. The permeability of the vasculature is a function, in large part, of complexes of proteins called adherens junctions that link cells together and to the actin cytoskeleton. These complexes are composed primarily of VE-cadherin and various adaptor and signaling proteins that form a tight, overlapping arrangement along the border of neighboring cells. Inflammatory stimuli (and other signals) can cause the break down of these junctions, thereby regulating vascular permeability and integrity. The primary VEGF receptor, VEGFR2 (KDR), is known to co-localize with these junctions in quiescent cells and induce permeability upon VEGF binding. VEGFR2-dependent signaling is in turn regulated by expression of another VEGF receptor, VEGFR1 (Flt-1), which acts as a VEGF sink to limit VEGFR2 activation. We set out to determine the role of VEGF in candidal invasion of human endothelial cells. We used an in vitro model of *Candida*-endothelial co-culture to determine changes in mRNA & protein levels, as well as protein localization and association.

C. albicans induces VEGF mRNA but inhibits VEGF signaling

Figure 1A. Quantitative RT-PCR data show that *C. albicans* induces significant increases in expression of VEGF, including transcripts encoding the primary secreted isoforms $VEGF_{121}$ & $VEGF_{165}$. This up regulation was found to be independent of VEGFR2 signaling as inhibition with SU5416 had no effect. Interestingly, using ELISA we found no detectable VEGF protein in cell supernatants (not shown) and no *Candida*-induced increase in activation of VEGFR2 in whole cell lysates.

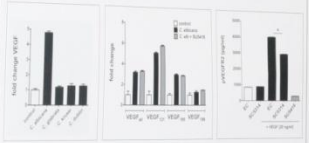

Figure 1B. Quantitative RT-PCR data show that *C. albicans* has no effect on the endothelial expression of the membrane-bound isoform of the negative regulator VEGFR1/mFlt-1, yet induces significant up regulation of the soluble, secreted isoform sFlt-1. Western blot data confirm no changes in cellular expression of mFlt-1 and ELISA results confirm the secretion of sFlt-1 in cell supernatants.

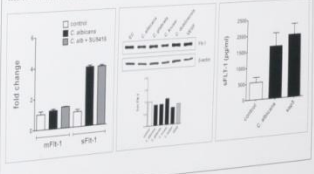

Candida disrupts cell-cell contacts

Figure 2. Although no changes in total VE-cadherin were detected by Western blot, *C. albicans* induced rapid dissolution of cell-cell contacts and actin bundles, as evidenced by immunocytochemistry.

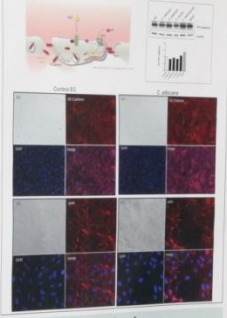

Conclusions

- *C. albicans* induces upregulation of VEGF mRNA isoforms $VEGF_{121}$ and $VEGF_{165}$ and this upregulation was VEGFR2-independent.
- Despite increased VEGF mRNA levels, *Candida* did not activate VEGF signaling and appears to inhibit VEGF-induced signaling, possibly through increasing the endothelial secretion of soluble Flt-1.
- Endothelial co-culture with *C.albicans* induced disruption of VE-cadherin complexes, resulting in formation of large intercellular gaps. Similarly, *Candida* induced rapid disassembly of cortical actin bundles and loss of cell superstructure.
- **We believe that *C. albicans*, in addition to causing direct cellular trauma, has significant negative impact on vascular integrity and vascular injury repair.**

16

LSUHealth NewOrleans HEALTH SCIENCES CENTER

Histologic Types and Risk Factors in Familial Lung Cancer Cases from Southern Louisiana

Matthew Haskins, Angelle Bencaz, Jessica Chambliss, Diptasri Mandal.
Department of Genetics, Louisiana State University Health Sciences Center

Introduction

Family Data

Results

Objectives

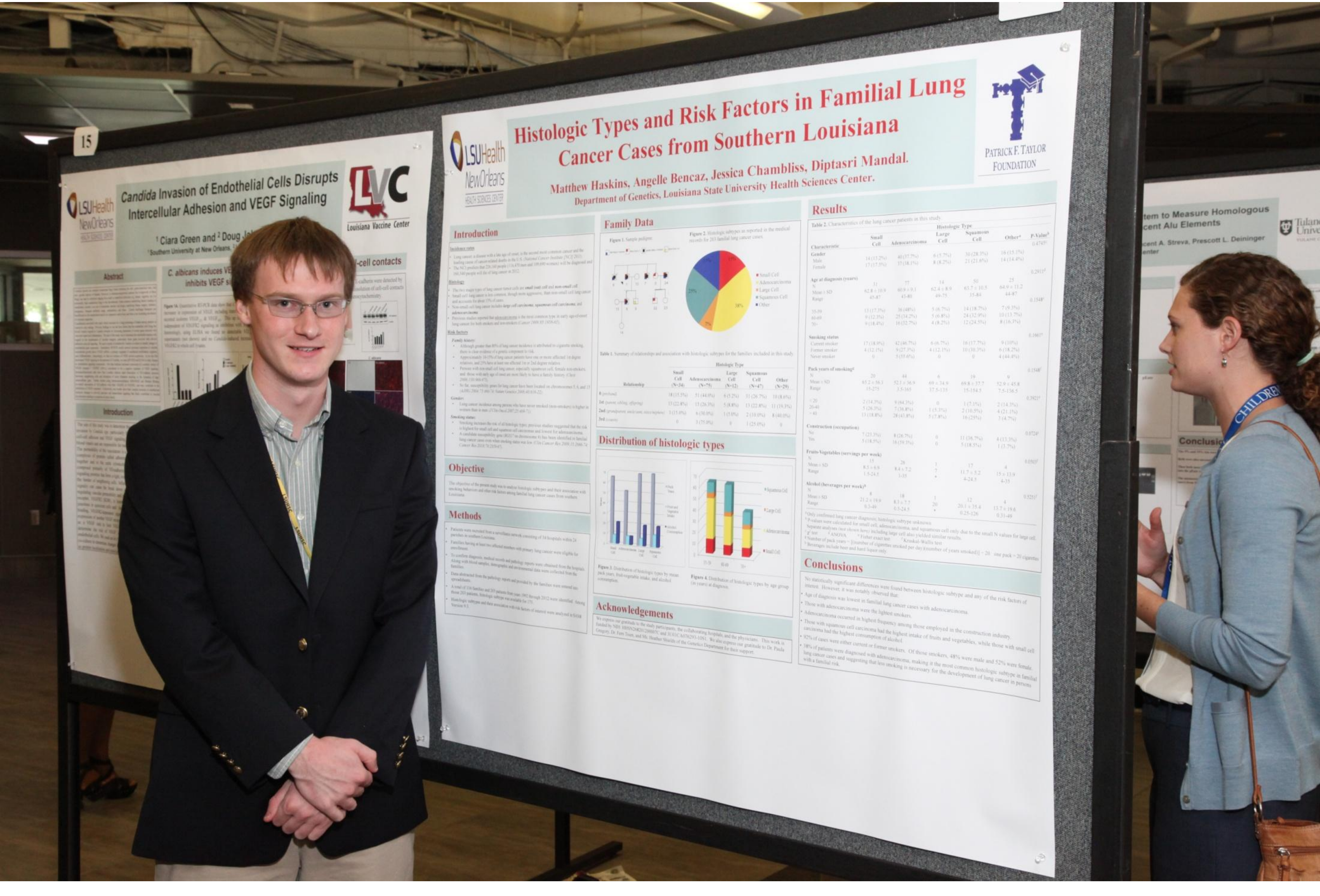
15
Candida Invasion of Endothelial Cells Disrupts
Intercellular Adhesion and VEGF Signaling
LSUHealth NewOrleans
Louisiana Vaccine Center
Abstract
Introduction
Histologic Types and Risk Factors in Familial Lung
Cancer Cases from Southern Louisiana
Matthew Haskins, Angelle Bencaz, Jessica Chambliss, Diptasri Mandal.
Department of Genetics, Louisiana State University Health Sciences Center.
PATRICK F. TAYLOR FOUNDATION
Introduction
Family Data
Results
Objective
Methods
Distribution of histologic types
Acknowledgements
Conclusions

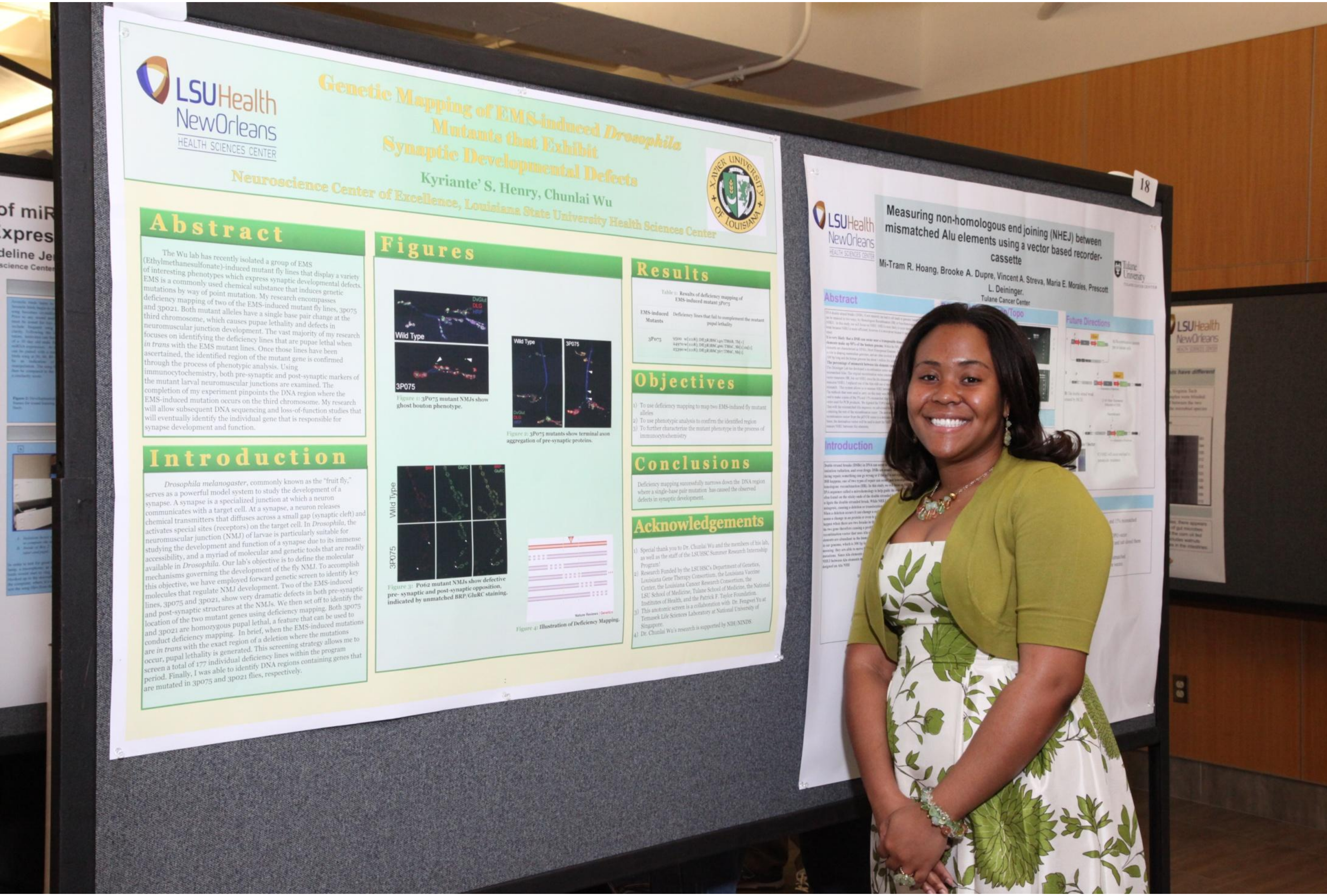
LSUHealth
NewOrleans
HEALTH SCIENCES CENTER
Genetic Mapping of EMS-induced Drosophila Mutants that Exhibit Synaptic Developmental Defects
Kyriante' S. Henry, Chunlai Wu
Neuroscience Center of Excellence, Louisiana State University Health Sciences Center
XAVIER UNIVERSITY OF LOUISIANA
Abstract
The Wu lab has recently isolated a group of EMS (Ethylmethanesulfonate)-induced mutant fly lines that display a variety of interesting phenotypes which express synaptic developmental defects. EMS is a commonly used chemical substance that induces genetic mutations by way of point mutation. My research encompasses deficiency mapping of two of the EMS-induced mutant fly lines, 3p075 and 3p021. Both mutant alleles have a single base pair change at the third chromosome, which causes pupae lethality and defects in neuromuscular junction development. The vast majority of my research focuses on identifying the deficiency lines that are pupae lethal when in trans with the EMS mutant lines. Once those lines have been ascertained, the identified region of the mutant gene is confirmed through the process of phenotypic analysis. Using immunocytochemistry, both pre-synaptic and post-synaptic markers of the mutant larval neuromuscular junctions are examined. The completion of my experiment pinpoints the DNA region where the EMS-induced mutation occurs on the third chromosome. My research will allow subsequent DNA sequencing and loss-of-function studies that will eventually identify the individual gene that is responsible for synapse development and function.
Introduction
Drosophila melanogaster, commonly known as the "fruit fly," serves as a powerful model system to study the development of a synapse. A synapse is a specialized junction at which a neuron communicates with a target cell. At a synapse, a neuron releases chemical transmitters that diffuses across a small gap (synaptic cleft) and activates special sites (receptors) on the target cell. In Drosophila, the neuromuscular junction (NMJ) of larvae is particularly suitable for studying the development and function of a synapse due to its immense accessibility, and a myriad of molecular and genetic tools that are readily available in Drosophila. Our lab's objective is to define the molecular mechanisms governing the development of the fly NMJ. To accomplish this objective, we have employed forward genetic screen to identify key molecules that regulate NMJ development. Two of the EMS-induced lines, 3p075 and 3p021, show very dramatic defects in both pre-synaptic and post-synaptic structures at the NMJs. We then set off to identify the location of the two mutant genes using deficiency mapping. Both 3p075 and 3p021 are homozygous pupal lethal, a feature that can be used to conduct deficiency mapping. In brief, when the EMS-induced mutations are in trans with the exact region of a deletion where the mutations occur, pupal lethality is generated. This screening strategy allows me to screen a total of 177 individual deficiency lines within the program period. Finally, I was able to identify DNA regions containing genes that are mutated in 3p075 and 3p021 flies, respectively.
Figures
Wild Type
3P075
Figure 1: 3P075 mutant NMJs show ghost bouton phenotype.
Figure 2: 3P075 mutants show terminal axon aggregation of pre-synaptic proteins.
Wild Type
3P075
Figure 3: P062 mutant NMJs show defective pre- synaptic and post-synaptic opposition, indicated by unmatched BRP/GluRC staining.
Figure 4: Illustration of Deficiency Mapping.
Results
Table 1: Results of deficiency mapping of EMS-induced mutant 3P075
EMS-induced Mutants
Deficiency lines that fail to complement the mutant pupal lethality
3P075
Objectives
1) To use deficiency mapping to map two EMS-induced fly mutant alleles
2) To use phenotypic analysis to confirm the identified region
3) To further characterize the mutant phenotype in the process of immunocytochemistry
Conclusions
Deficiency mapping successfully narrows down the DNA region where a single-base pair mutation has caused the observed defects in synaptic development.
Acknowledgements
1) Special thank you to Dr. Chunlai Wu and the members of his lab, as well as the staff of the LSUHSC Summer Research Internship Program!
2) Research Funded by the LSUHSC's Department of Genetics, Louisiana Gene Therapy Consortium, the Louisiana Vaccine Center, the Louisiana Cancer Research Consortium, the LSU School of Medicine, Tulane School of Medicine, the National Institutes of Health, and the Patrick F. Taylor Foundation.
3) This anatomic screen is a collaboration with Dr. Fengwei Yu at Temasek Life Sciences Laboratory at National University of Singapore.
4) Dr. Chunlai Wu's research is supported by NIH/NINDS.
18
LSUHealth
NewOrleans
HEALTH SCIENCES CENTER
Measuring non-homologous end joining (NHEJ) between mismatched Alu elements using a vector based recorder-cassette
Mi-Tram R. Hoang, Brooke A. Dupre, Vincent A. Streva, Maria E. Morales, Prescott L. Deininger.
Tulane Cancer Center
Tulane University
Abstract
Introduction
Future Directions

17

Genetic Mapping of EMS-induced Drosophila Mutants that Exhibit Synaptic Developmental Defects

Kyriante' S. Henry, Chunlai Wu

Neuroscience Center of Excellence, Louisiana State University Health Sciences Center

Abstract

Introduction

Figures

Results

Objectives

Measuring non-homologous end joining (NHEJ) between mismatched Alu elements using a vector based recorder-cassette

Mi-Tram R. Hoang, Brooke A. Dupre, Vincent A. Streva, Maria E. Morales, Prescott L. Deininger.

Tulane Cancer Center

LSUHealth NewOrleans HEALTH SCIENCES CENTER

Tulane University TULANE CANCER CENTER

Abstract

DNA double strand breaks (DSB), if not repaired, can lead to cell death or genomic instability. A DSB can be repaired in two ways by Homologous Recombination (HR) or Non-Homologous End Joining (NHEJ). In this study we will focus on NHEJ. NHEJ is more likely to occur during a double strand break because NHEJ is more efficient, however, it is error prone because it can cause deletions during break repair.

It is very likely that a DSB can occur near a transposable element because transposable elements make up 80% of the human genome. Within the 80%, 11% are Alu elements. Alu elements are characterized as SINEs. Short Interspersed Elements. SINEs are retrotransposons that play a role in shaping mammalian genomes, and are often involved in the repair of DSBs. All Alus are about 300 by long and the human genome has about 1 million Alu copies, which is 11% of the total genome.

The percentage of mismatch between Alu elements range from 5% to 30%.

The Deininger Lab has developed a recombination vector capable of measuring NHEJ between mismatched Alus. The original recombination vector consisted of two Alus with 5% mismatch. This vector measures HR, but not NHEJ, since the Alu elements are perfectly matched. To make a vector that measures NHEJ, I replaced one of the Alus with one of two different Alus, containing 5% or 15% mismatch. The system allows us to measure NHEJ between the Alu elements.

The methods that were used to carry out this study were PCR, sub-cloning, and LR cloning. PCR was used to make copies of the 5% and 15% mismatched Alus to put in the vector TOPO, which is a specific vector used for PCR products. We digested the TOPO vector to obtain the mismatched Alu sequence. Then with the mismatched Alu sequence, we sub-cloned the 5% and the 15% into a pUC19 vector containing the rest of the recombination vector. The next step was to transfer the mismatch recombination vector from the pUC19 vector to a destination vector using the gateway system. In the future, the destination vector will be used to insert the NHEJ recombination vector into cell lines to measure NHEJ between Alu elements.

Introduction

Double strand breaks (DSBs) in DNA can occur in many ways; DNA polymerase errors, restriction radiation, and even drugs. DSBs are usually dangerous when they occur because during repair, something can go wrong or if the cell is not repaired, the cell can die. When a DSB happens, one of two types of repair can occur: non homologous end joining (NHEJ) or homologous recombination (HR). In this study, we will focus on NHEJ. NHEJ uses a short DNA sequence called a microhomology to help guide the repair. These microhomologies are often found on the sticky ends of the double-stranded break and are usually the quickest way to ligate the double stranded break. While NHEJ is efficient and quick, it can be very mutagenic, causing a deletion or translocation, thus being very dangerous during a repair. When a deletion occurs it can change a codon which are three nucleotides long- which means a change in an protein or even to put a stop codon in the sequence. Translocation can happen when there are two breaks in the DNA and NHEJ tries to repair it but it mixes up the two gene therefore causing a problem, such as cancer. In this study, we use a recombination vector that uses Alu elements to study how NHEJ may lead to cancer. Alu elements are abundant in the human genome. We have approximately 1 million Alu elements in our genome, which is 300 by long in length. Alu elements are transposable elements meaning, they are able to move themselves and the movement of the Alu element can cause mutations. Since Alu elements are abundant and breaks often occur near Alu elements, NHEJ between Alu elements may result in disease. To study NHEJ between Alu elements, we designed an Alu NHJ.

PCR/Gel Extraction/Topo

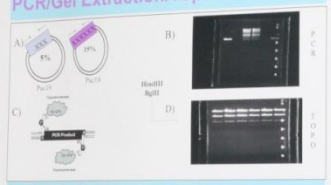

Sub-Cloning

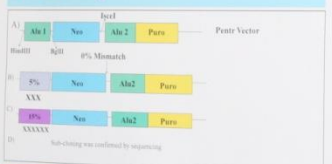

LR Clonase

Future Directions

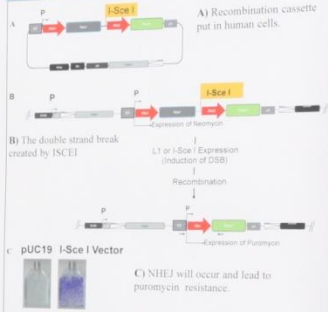

Conclusions

I successfully PCR amplified the 5% and 15% mismatched Alus

I cloned both mismatched Alus into a TOPO vector

I digested the inserted Alus out of TOPO and sub cloned them into an entry vector

I used LR clonase to transfer the new mismatched recombination cassette into a destination vector.

22

Linkage Analyses

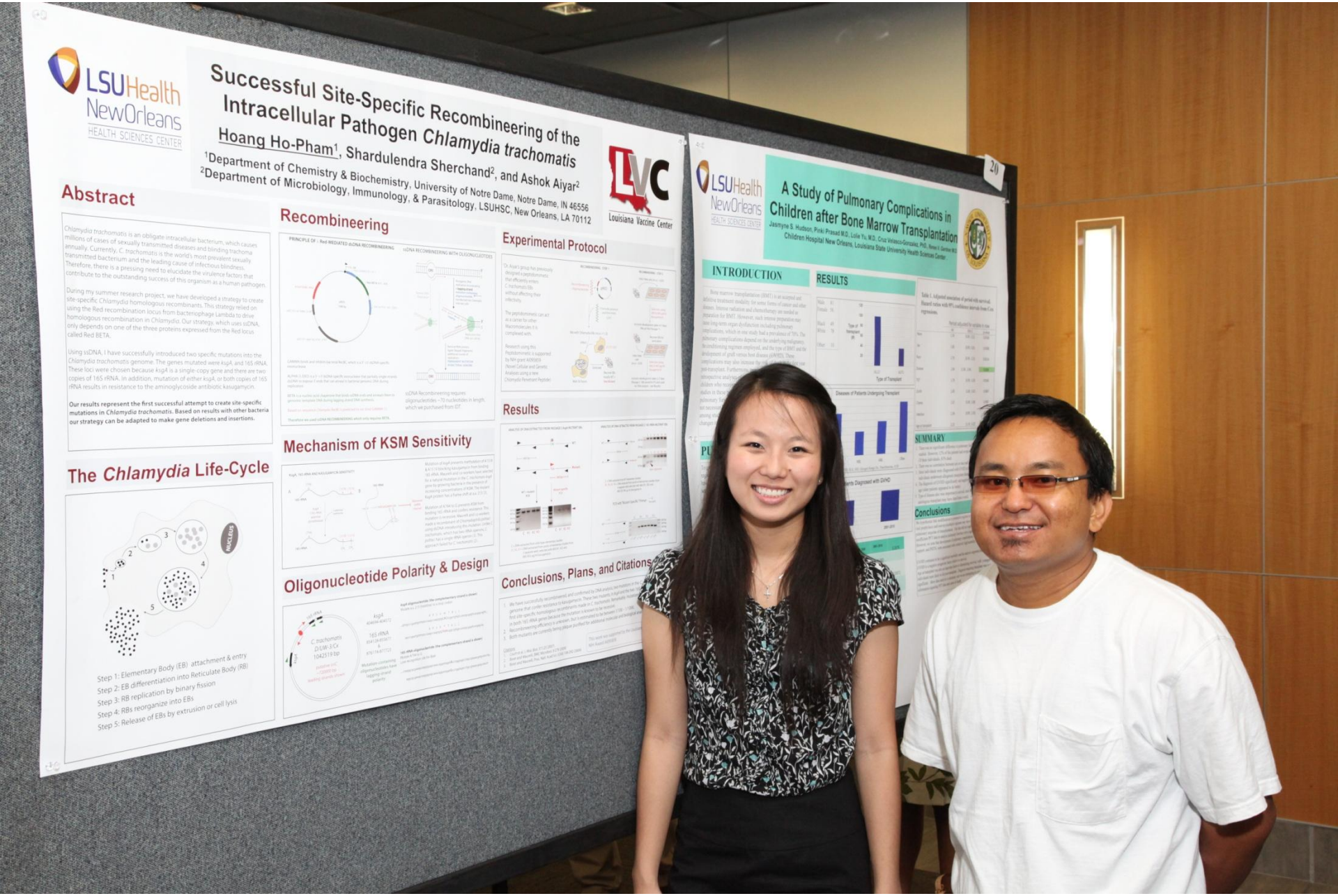
LSUHealth NewOrleans
HEALTH SCIENCES CENTER
Successful Site-Specific Recombineering of the Intracellular Pathogen Chlamydia trachomatis
Hoang Ho-Pham[1], Shardulendra Sherchand[2], and Ashok Aiyar[2]
[1]Department of Chemistry & Biochemistry, University of Notre Dame, Notre Dame, IN 46556
[2]Department of Microbiology, Immunology, & Parasitology, LSUHSC, New Orleans, LA 70112
LVC
Louisiana Vaccine Center
Abstract
Chlamydia trachomatis is an obligate intracellular bacterium, which causes millions of cases of sexually transmitted diseases and blinding trachoma annually. Currently, C. trachomatis is the world's most prevalent sexually transmitted bacterium and the leading cause of infectious blindness. Therefore, there is a pressing need to elucidate the virulence factors that contribute to the outstanding success of this organism as a human pathogen.
During my summer research project, we have developed a strategy to create site-specific Chlamydia homologous recombinants. This strategy relied on using the Red recombination locus from bacteriophage Lambda to drive homologous recombination in Chlamydia. Our strategy, which uses ssDNA, only depends on one of the three proteins expressed from the Red locus called Red BETA.
Using ssDNA, I have successfully introduced two specific mutations into the Chlamydia trachomatis genome. The genes mutated were ksgA and 16S rRNA. These loci were chosen because ksgA is a single-copy gene and there are two copies of 16S rRNA. In addition, mutation of either ksgA, or both copies of 16S rRNA results in resistance to the aminoglycoside antibiotic kasugamycin.
Our results represent the first successful attempt to create site-specific mutations in Chlamydia trachomatis. Based on results with other bacteria our strategy can be adapted to make gene deletions and insertions.
The Chlamydia Life-Cycle
NUCLEUS
Step 1: Elementary Body (EB) attachment & entry
Step 2: EB differentiation into Reticulate Body (RB)
Step 3: RB replication by binary fission
Step 4: RBs reorganize into EBs
Step 5: Release of EBs by extrusion or cell lysis
Recombineering
Mechanism of KSM Sensitivity
Oligonucleotide Polarity & Design
Experimental Protocol
Results
Conclusions, Plans, and Citations
20
LSUHealth NewOrleans
HEALTH SCIENCES CENTER
A Study of Pulmonary Complications in Children after Bone Marrow Transplantation
Jasmyne S. Hudson, Pinki Prasad M.D., Lolie Yu, M.D., Cruz Velasco-Gonzalez, PhD., Renee V. Gardner M.D.
Children Hospital New Orleans, Louisiana State University Health Sciences Center
INTRODUCTION
RESULTS
SUMMARY
Conclusions

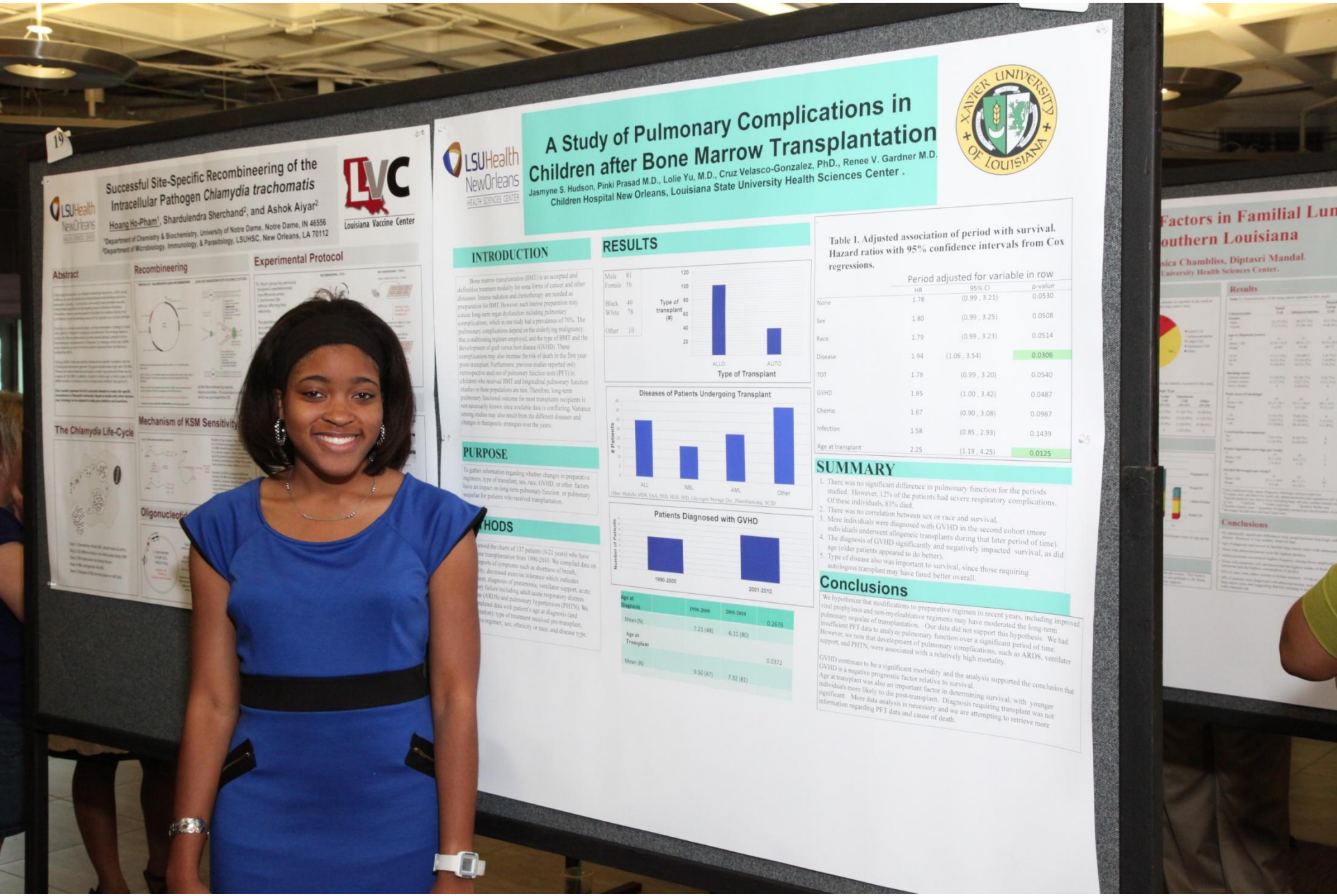
19
Successful Site-Specific Recombineering of the Intracellular Pathogen Chlamydia trachomatis
Hoang Ho-Pham[1], Shardulendra Sherchand[2], and Ashok Aiyar[2]
[1]Department of Chemistry & Biochemistry, University of Notre Dame, Notre Dame, IN 46556
[2]Department of Microbiology, Immunology, & Parasitology, LSUHSC, New Orleans, LA 70112
Louisiana Vaccine Center
Abstract
Recombineering
Experimental Protocol
The Chlamydia Life-Cycle
Mechanism of KSM Sensitivity
A Study of Pulmonary Complications in Children after Bone Marrow Transplantation
Jasmyne S. Hudson, Pinki Prasad M.D., Lolie Yu, M.D., Cruz Velasco-Gonzalez, PhD., Renee V. Gardner M.D.
Children Hospital New Orleans, Louisiana State University Health Sciences Center .
XAVIER UNIVERSITY OF LOUISIANA
INTRODUCTION
Bone marrow transplantation (BMT) is an accepted and definitive treatment modality for some forms of cancer and other diseases. Intense radiation and chemotherapy are needed as preparation for BMT. However, such intense preparation may cause long-term organ dysfunction including pulmonary complications, which in one study had a prevalence of 70%. The pulmonary complications depend on the underlying malignancy, the conditioning regimen employed, and the type of BMT and the development of graft versus host disease (GVHD). These complications may also increase the risk of death in the first year post-transplant. Furthermore, previous studies reported only retrospective analyses of pulmonary function tests (PFT) in children who received BMT and longitudinal pulmonary function studies in these populations are rare. Therefore, long-term pulmonary functional outcome for most transplants recipients is not necessarily known since available data is conflicting. Variance among studies may also result from the different diseases and changes in therapeutic strategies over the years.
PURPOSE
To gather information regarding whether changes in preparative regimens, type of transplant, sex, race, GVHD, or other factors have an impact on long-term pulmonary function or pulmonary sequelae for patients who received transplantation.
HODS
rewed the charts of 137 patients (0-21 years) who have ne transplantation from 1990-2010. We compiled data on eports of symptoms such as shortness of breath, y, decreased exercise tolerance which indicates ssic diagnosis of pneumonia, ventilator support, acute ary failure including adult/acute respiratory distress e (ARDS) and pulmonary hypertension (PHTN). We ulated data with patient's age at diagnosis (and ation), type of treatment received pre-transplant, e regimen; sex, ethnicity or race, and disease type.
RESULTS
Male 81
Female 56
Black 49
White 78
Other 10
Type of transplant (#)
ALLO
AUTO
Type of Transplant
Diseases of Patients Undergoing Transplant
Patients
ALL
NBL
AML
Other
Other: Medellin, MDS, SAA, SMD, HLH, JHD, Glycogen Storage Dis., Pancoblastoma, SCID
Patients Diagnosed with GVHD
Number of Patients
1990-2000
2001-2010
Age at Diagnosis
1990-2000
2001-2010
Mean (N)
7.21 (48)
6.11 (80)
0.2676
Age at Transplant
Mean (N)
9.50 (47)
7.32 (81)
0.0372
Table 1. Adjusted association of period with survival. Hazard ratios with 95% confidence intervals from Cox regressions.
Period adjusted for variable in row
HR
95% CI
p-value
None 1.78 (0.99 , 3.21) 0.0530
Sex 1.80 (0.99 , 3.25) 0.0508
Race 1.79 (0.99 , 3.23) 0.0514
Disease 1.94 (1.06 , 3.54) 0.0306
TOT 1.78 (0.99 , 3.20) 0.0540
GVHD 1.85 (1.00 , 3.42) 0.0487
Chemo 1.67 (0.90 , 3.08) 0.0987
Infection 1.58 (0.85 , 2.93) 0.1439
Age at transplant 2.25 (1.19 , 4.25) 0.0125
SUMMARY
1. There was no significant difference in pulmonary function for the periods studied. However, 12% of the patients had severe respiratory complications. Of these individuals, 83% died.
2. There was no correlation between sex or race and survival.
3. More individuals were diagnosed with GVHD in the second cohort (more individuals underwent allogeneic transplants during that later period of time).
4. The diagnosis of GVHD significantly and negatively impacted survival, as did age (older patients appeared to do better).
5. Type of disease also was important to survival, since those requiring autologous transplant may have fared better overall.
Conclusions
We hypothesize that modifications to preparative regimen in recent years, including improved viral prophylaxis and non-myeloablative regimens may have moderated the long-term pulmonary sequelae of transplantation. Our data did not support this hypothesis. We had insufficient PFT data to analyze pulmonary function over a significant period of time. However, we note that development of pulmonary complications, such as ARDS, ventilator support, and PHTN, were associated with a relatively high mortality.
GVHD continues to be a significant morbidity and the analysis supported the conclusion that GVHD is a negative prognostic factor relative to survival.
Age at transplant was also an important factor in determining survival, with younger individuals more likely to die post-transplant. Diagnosis requiring transplant was not significant. More data analysis is necessary and we are attempting to retrieve more information regarding PFT data and cause of death.
Factors in Familial Lun
outhern Louisiana
sica Chambliss, Diptasri Mandal
University Health Sciences Center.
Results
Conclusions

21

LSU Health New Orleans
HEALTH SCIENCES CENTER

Roles of miRNA in Regulating FOXP2 Expression in Zebra Finch

Madeline Jenkins, Zhimin Shi, Xiao Ching Li
Neuroscience Center, Louisiana State University Health Sciences Center

LSU Health New Orleans

Abstract

Mutations of the FOXP2 gene cause language disorders. FOXP2 controls expression of several hundred genes which are important for the development of neural circuits. The zebra finch shares many parallels with speech and language development in humans, we are able to study the birds' vocal development time frame and apply our findings to language disorders in humans. We try to study how miRNA regulates FOXP2 and why FOXP2 regulates vocal learning in juvenile zebra finch. In our experiment, we inject lentivirus into Area X, an area of the forebrain containing high levels of FOXP2, into a juvenile finch brain. Lentivirus is used to change miRNA expression. This will allow us to detect FOXP2 protein changes, observe the song learning for finch and analyze the song behavior during song development. This process will be used to find one or two miRNAs which can regulate vocal learning and song behavior. In order for the young bird, the pupil, to learn the song of the zebra finch, he must be paired with an older male bird, the tutor. Only the males can sing. In our experiment, we set up an isolation box. In this box, we set up a microphone to record all of the sounds made by the bird and also a lamp with a 12 hour on/off cycle. We recorded the bird's sound from 8 a.m. to 12 p.m. First, I had to sort the song files from the background noises. I chose 20 song motifs randomly to score. Using the sound analysis software, I compared the tutor's song motifs in order to get a variability score. The files were analyzed on the syllable and motif levels. Motifs are made up of syllables. With these scores, we will be able to compare the variability of the tutor and pupil's song post-injection. This whole process will be used to find which miRNAs regulate FOXP2 expression.

Introduction

Song learning in zebra finch shares many parallels with speech and language development in humans. Because the FOXP2 gene is highly conserved between humans and zebra finches, we are able to use the zebra finchs' vocal development as a model to study human language development and apply our research findings to language disorders in humans. In the zebra finch brain, FOXP2 is expressed in Area X, a forebrain basal ganglia nucleus required for vocal learning. An adequate FOXP2 expression is needed for normal sound development. Reduced FOXP2 expression leads to structural and functional abnormalities of the brain. How FOXP2 is regulated is not understood. Recently the Li laboratory used sequence analyses to identify several miRNAs, including miR-9, that could potentially regulate FOXP2. Based on these findings, we hypothesize miR-9 is a fundamental regulator of FOXP2 gene expression. To test this hypothesis, the lab plans to use lentivirus to manipulate miRNA expression in Area X and test the sound-learning process of the juvenile zebra finches.


Male zebra finch


Female zebra finch


Juvenile zebra finch

Background

Juvenile birds learn to sing from adult tutors. Juvenile birds begin to sing at 10 days of age. The song becomes crystallized by 90 days of age. Prior to any sound analysis, all potential tutors must be tested for two qualities. These qualities include frequency, song production and sound clarity. Following the identification of suitable tutors, lentivirus can then be injected into Area X of a 30 day old male finch brain to manipulate miRNA expression. At that point, a juvenile bird can be paired with a tutor and recordings of the birds song at 50, 60, 80 and 100 days of age will be an indication of the effects miRNA manipulation. The song files from those days will then be compared to the tutors song to determine a similarity score.

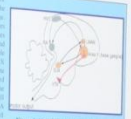
Figure 1: Neural circuits for sound behavior in a zebra finch brain.


Figure 2: Developmental time frames for sound learning in zebra finch.

Methods


A

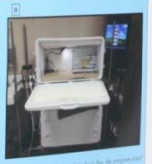
B

A. Isolation boxes set up with computer. Computer contains Sound Analysis Pro, the program used to compare the tutor and pupils sound.
B. Inside of Box 2. Contains lamp with a timer, microphone, air tube, and the bird cage containing tutor and pupil.

In order to test for good tutors we put adult male finches in isolation boxes. These boxes contain a timed lamp, a microphone on an tube, and the bird cage. The lamp has a 12 hour on/off cycle. Typically, the birds would start to sing in the mornings when the lights come on. At night there was little to no sound. I hooked up to the microphone in an audio box that receives the sound from the microphone and which it to the computer, where it's stored. Using the sound analysis software installed on the computer, I was able to sort the song files from the background noises.

Scoring

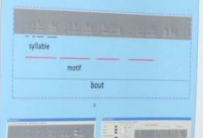

Conclusions

22

LSU Health New Orleans

"Prostate Cancer Genetics: How Informative is Your Family?"

Brianne Jones, Elisa Ledet and Diptasri Mandal.
Louisiana State University Health Sciences Center-New Orleans.

Introduction

Family Data

Results: Linkage Analyses

Conclusions

aps

Nuts about your gut?
Does walnut consumption influence n
gut flora?

Shelia D. Banks, Lauri O. Byerley, Pl
American Physiology Association, LSU Health Sciences Cent

About Gut Flora

Hypothesis
Consumption of a diet rich in walnuts will change the species of gut microbes compared to a diet rich in corn oil (AKA the American diet)

Experimental Design

Atenolol Nanoparticles
Magrath, Richard A. Graves, Tarun
of Pharmacy, Xavier University of Louisiana, New Orlean

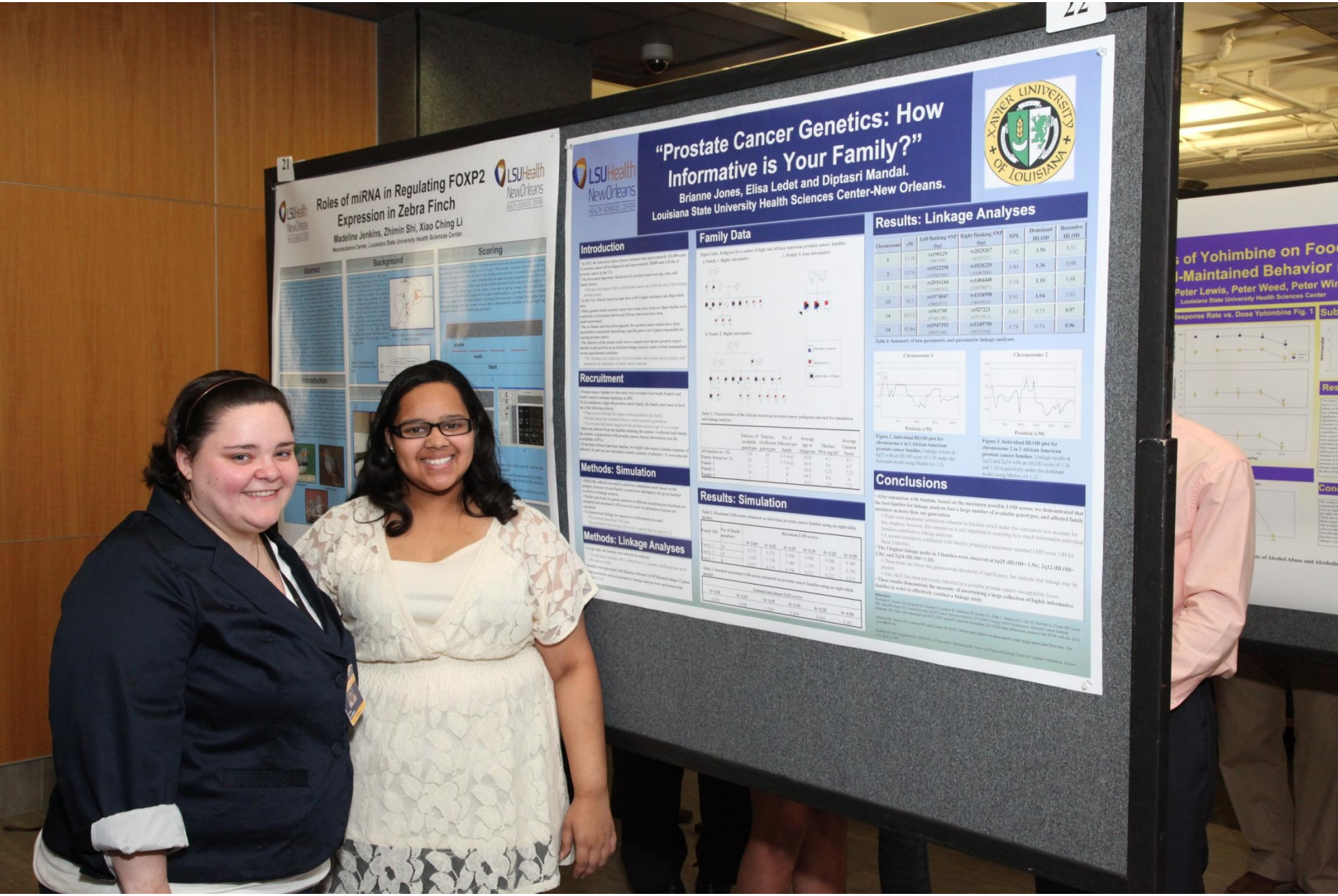
21
Roles of miRNA in Regulating FOXP2 Expression in Zebra Finch
Madeline Jenkins, Zhimin Shi, Xiao Ching Li
Neuroscience Center, Louisiana State University Health Sciences Center
LSUHealth New Orleans
Abstract
Background
Scoring
Introduction
22
"Prostate Cancer Genetics: How Informative is Your Family?"
Brianne Jones, Elisa Ledet and Diptasri Mandal.
Louisiana State University Health Sciences Center-New Orleans.
XAVIER UNIVERSITY OF LOUISIANA
Introduction
Family Data
Results: Linkage Analyses
Recruitment
Methods: Simulation
Methods: Linkage Analyses
Results: Simulation
Conclusions
of Yohimbine on Food
-Maintained Behavior
Peter Lewis, Peter Weed, Peter Wi
Louisiana State University Health Sciences Center
Response Rate vs. Dose Yohimbine Fig. 1

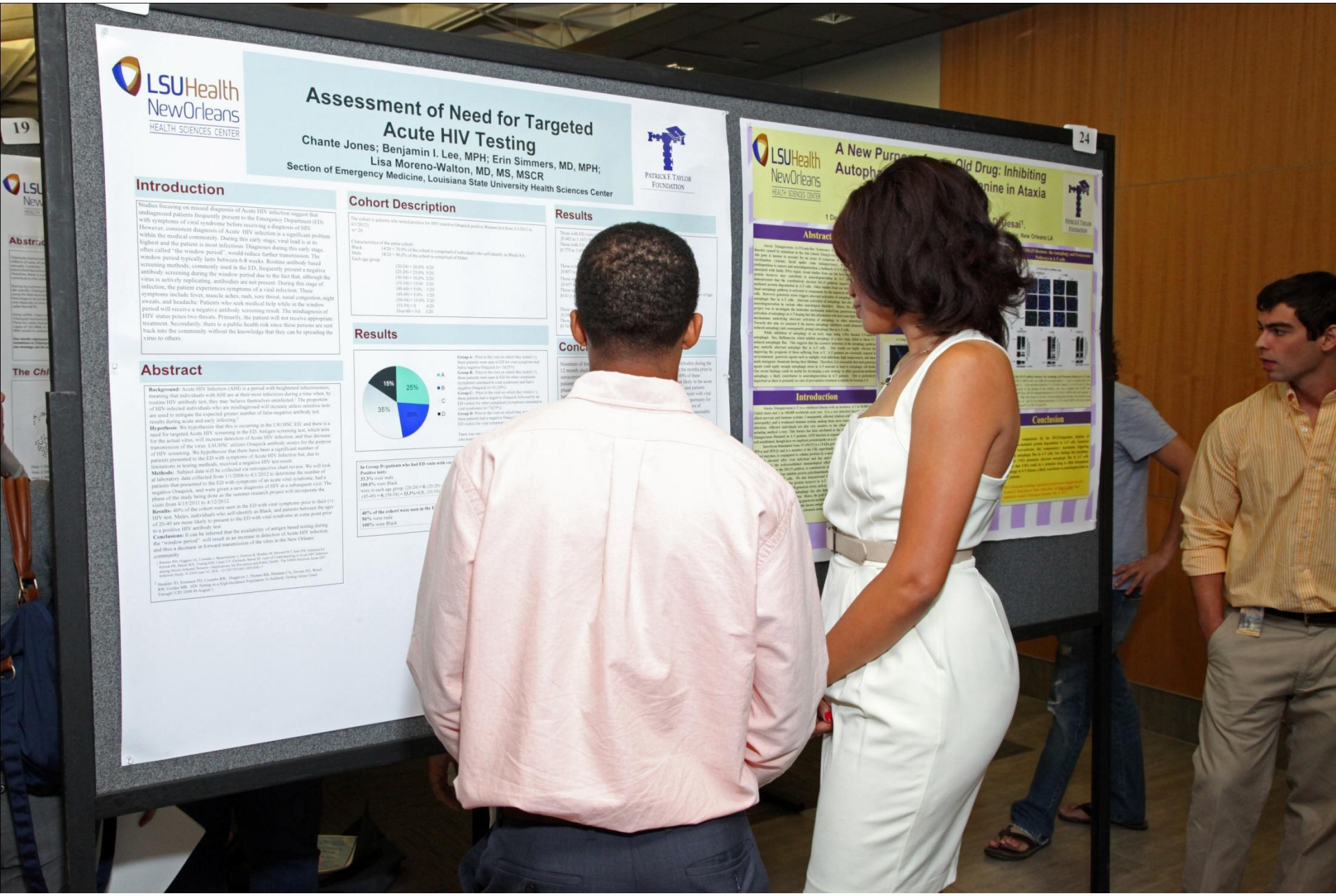
LSUHealth NewOrleans
HEALTH SCIENCES CENTER
Assessment of Need for Targeted Acute HIV Testing
Chante Jones; Benjamin I. Lee, MPH; Erin Simmers, MD, MPH; Lisa Moreno-Walton, MD, MS, MSCR
Section of Emergency Medicine, Louisiana State University Health Sciences Center
PATRICK F. TAYLOR FOUNDATION
Introduction
Studies focusing on missed diagnosis of Acute HIV infection suggest that undiagnosed patients frequently present to the Emergency Department (ED) with symptoms of viral syndrome before receiving a diagnosis of HIV. However, consistent diagnosis of Acute HIV infection is a significant problem within the medical community. During this early stage, viral load is at its highest and the patient is most infectious. Diagnoses during this early stage, often called "the window period", would reduce further transmission. The window period typically lasts between 6-8 weeks. Routine antibody based screening methods, commonly used in the ED, frequently present a negative antibody screening during the window period due to the fact that, although the virus is actively replicating, antibodies are not present. During this stage of infection, the patient experiences symptoms of a viral infection. These symptoms include fever, muscle aches, rash, sore throat, nasal congestion, night sweats, and headache. Patients who seek medical help while in the window period will receive a negative antibody screening result. The misdiagnosis of HIV status poses two threats. Primarily, the patient will not receive appropriate treatment. Secondarily, there is a public health risk since these persons are sent back into the community without the knowledge that they can be spreading the virus to others.
Abstract
Cohort Description
Results
Results
15%
25%
35%
A
B
C
D
24
LSUHealth NewOrleans
HEALTH SCIENCES CENTER
Abstract
Introduction
Conclusion


23
LSUHealth
NewOrleans
HEALTH SCIENCES CENTER
Assessment of Need for Targeted Acute HIV Testing
Chante Jones; Benjamin I. Lee, MPH; Erin Simmers, MD, MPH; Lisa Moreno-Walton, MD, MS, MSCR
Section of Emergency Medicine, Louisiana State University Health Sciences Center
PATRICK F. TAYLOR FOUNDATION
Introduction
Cohort Description
Results
Results
Conclusions
Abstract
Discussion
Acknowledgments
24
A New Purpose for an Old Drug: Inhibiting Autophagy with 3-Methyladenine in Ataxia Telangiectasia
Recombineering
Mechanism